High-voltage nanosecond discharge in a dense gas at a high overvoltage with runaway electrons

L. P. Babich, T. V. Loĭko, and V. A. Tsukerman

All-Union Scientific-Research Institute of Experimental Physics, Arzamas, Gor'kiĭ Oblast'
Usp. Fiz. Nauk **160**, 49–82 (July 1990)

The concepts of local and nonlocal models of the breakdown of dense gases are introduced. The basis for a nonlocal model with runaway electrons is discussed. Experimental results on electric discharges in dense gases which develop in a regime of intense electron runaway, in contrast with the classical forms of gas discharges, are reviewed. It is shown that electron runaway plays a fundamental role in the breakdown dynamics of dense gases over a wide range of conditions. Space-time and energy characteristics of the pulses of runaway electrons and of the accompanying x radiation are reported. The involvement of runaway electrons in the breakdown mechanism can be seen in a shift of the minimum on the $U(Pd)$ curves toward higher values of Pd as the overvoltage increases. When the overvoltage reaches a large factor, a polarization self-acceleration, as discussed by Askar'yan, occurs, and runaway electrons with energies $\varepsilon > eU_{\max}$ are generated. The breakdown of a dense gas in a strong field differs from that at a moderate overvoltage in that it ceases to be a purely volume process.

1. INTRODUCTION

The breakdown of gases at pressures from tens to thousands of Torr by nanosecond-range high-voltage pulses has been under study for five decades now, beginning with the pioneering studies by Neuman[1] and Fletcher.[2] Progress in the technology of nanosecond high-voltage pulses in the 1960s attracted increased interest to nanosecond discharges in gases. Despite the rapid growth in the number of experimental studies[3,4] and in technical applications[5–8] of nanosecond gas discharges, the advance to a new time scale was not accompanied by a corresponding reexamination of the fundamental ideas of the classical breakdown models, which had been developed for approximately static conditions.[9–12] This is true despite the fact that in a review many years ago Mesyats *et al.*[3] pointed out that gas discharges at the nanosecond time scale have some qualitatively new aspects. Although the various models for the breakdown of dense gases differ in many ways, sometimes radically, they do have one common fundamental feature: They are "local" models in the sense that the values of such average quantities as the electron energy $\langle\varepsilon\rangle$, the directed velocity v_- and the Townsend ionization coefficient α at a given space-time point $(\mathbf{r},t)$ are determined by the local field at the same point, $\mathbf{E}(\tau,t) = \mathbf{E}_0 + \mathbf{E}_p(\mathbf{r},t)$, where $\mathbf{E}_0$ and $\mathbf{E}_p = \mathbf{E}_{p^+} + \mathbf{E}_{p^-}$ are the external field and the space-charge field. Among the local models are Townsend's model of the multiple generation of avalanches involving γ processes at the cathode and the various modifications of the single-avalanche streamer model of Meek, Loeb, and Raether.[9–12] The latter model is invoked to describe the breakdown of dense gases on the right-hand branch of the Paschen curve $[Pd \gg (Pd)_{\min}]$ in cases in which the length scale (z_{cr}) and time scale (t_{cr}) of the development of the avalanche to a critical size according to the Meek or Raether criterion satisfies the relations

$$z_{cr} = \alpha^{-1} \ln N_e^{cr} \leqslant d, \qquad t_{cr} \leqslant \frac{d}{v_-}, \tag{1}$$

where $N_e^{(cr)}$ is the number of electrons in a critical avalanche, and d is the distance between electrodes. In a classical streamer model one can distinguish three basic ideas: (1) The field is intensified at the fronts of electron avalanches and streamers because of their polarization $(E_f = E_0 + E_{p\pm})$. (2) A preionization of the gas is caused ahead of the fronts by photons with energies $\hbar\omega \approx \varepsilon_i$, where ε_i is the ionization potential. (3) The governing process in the breakdown mechanism is ionization in the gas volume; emission from the cathode is inconsequential. As a result of this field intensification, the electron energy becomes far higher than the quantity $\langle\varepsilon(E_0)\rangle$, where E_0 is the equilibrium value of the external field. As a result, ionization processes intensify. Volume photoionization is used to explain the high streamer propagation velocities $\gg 6v_-(E_0)$, and it is of fundamental importance for the propagation of a streamer toward the cathode. The photoionizing radiation was studied experimentally and identified in Refs. 13–17, among other places. A question which remains a matter of debate is the nature of the radiation which initiates secondary ionization centers outside the volume of the primary avalanche.[9,10,12,18–20] In gas mixtures, transparency windows exist, and the emission by certain components ionizes others.[9,21,22] The streamer model has been interpreted most clearly by Lovanskiĭ and Firsov,[12] according to whom secondary avalanches are initiated in an associative ionization reaction $A + A^* \to A_2^+ + e^-$ involving excited atoms A^* which are generated by long-range photons with $\hbar\omega < \varepsilon_i$ emitted in the line wings. In molecular gases, however, the energy of the first excited state which is capable of participating in this reaction differs only slightly from ε_i (Ref. 19), and the number of photons emitted from the primary avalanche is definitely too small. An alternative explanation is photoionization by recombination photons with[18,20] $\hbar\omega > \varepsilon_i$, but the latter are strongly absorbed in a dense gas and do not escape from the volume of the primary avalanche. They are not detected in the breakdown state,[23,24] possibly because of limitations imposed by the sensitivity of the measurement instruments. Note should also be taken of attempts to construct a phonon-free mechanism for streamer propagation, on the basis of plasma waves.[25,26] It is fair to say that the various modifications of the streamer model are today generally accepted for describing the breakdown of dense gases at relatively low overvoltages $(\Delta \ll 1)$, although the analytic and numerical studies have had to be restricted to

 0038-5670/90/070521-20$01.00

an enumeration of possible photon emission mechanisms which would be capable of ionizing a gas over large distances, without the assignment of a preference to any one of these mechanisms[19] (the "overvoltage" is to be understood here as the quantity $\Delta = U_m/U_s - 1$, where $U_m \leqslant U_r^m$ is the maximum value of the voltage pulse $U(t)$ across the electrode gap, U_{gen}^m is the maximum value of the pulse from the generator under open-circuit conditions, and U_s is the static breakdown voltage of the given gap).

If the overvoltage is sufficiently high ($\Delta \gtrsim 1$), the breakdown of a dense gas and the development of the entire gas-discharge process take a course different from that of classical discharges. The discrepancy with the generally accepted local models becomes particularly obvious at $\Delta \gg 1$. As Δ is increased, the scale values z_{cr} and t_{cr} decrease rapidly, and at $\Delta \gg 1$ the energy of the directed motion of the electrons becomes comparable to the total kinetic energy. An extrapolation of the first of the three streamer-model ideas listed above into the strong-field region unavoidably leads to the conclusion that "runaway" electrons (REs) can be produced at the front of a streamer under the condition $E_0 < E_{cr}$, where E_{cr} is the critical field, which causes a continuous acceleration of electrons beginning at thermal energies $T_e \approx 1$–10 eV (Ref. 27). Starting at certain sufficiently high values of E_0, the displacement of the field to the streamer front as a result of its polarization occurs over a time of the order of the time of motion of the runaway electrons near the front. The result is a synchronized motion of the region of strengthened fringing field and of the accelerated electrons.[28-30] With increasing Δ, the emission of photons from the avalanches decreases sharply.[3] In addition, at $\Delta \gg 1$ the second of the three streamer-model ideas is not of fundamental importance, since the runaway electrons give the ionized region a high propagation velocity toward the anode. The accompanying x radiation preionizes the gas and causes a photoelectric effect at the cathode, thereby causing a motion of the ionization front toward the cathode. Finally, since breakdown is initiated by field emission[3,4,31] under the condition $\Delta \gg 1$, and the primary avalanche becomes critical near the point of initiation ($d \gg z_{cr} \approx \mu$m), there is a self-consistent intensification of the field of the positive space charge, E_p, and of the field emission.[32] At $\Delta \gg 1$, emission processes thus play a fundamental role in the propagation of the ionization toward the cathode.

The high penetrating capability of the runaway electrons and of the x radiation results in an ionization of dense gases far from the primary ionization centers. As a result, the discharge loses its spatially compact form, acquiring a diffuse or multichannel nature. At the same time, those breakdown models which assume a buildup of space charge in the form of spatially compact regions, with dimensions determined primarily by diffusion and collective electrostatic space-charge forces, become meaningless. The participation of runaway electrons in the breakdown of dense gases implies that an appropriate breakdown model would be a substantially nonlocal model. This idea of a nonlocal model was developed to some extent in Refs. 27 and 34–39, although the question of a nonlocal value of α at high values of E_0/P has been discussed even earlier by Granovskiĭ,[40] in a study of an externally sustained current in a gas-filled gap with small values of Pd. That model, being based on a purely electron kinetics, is attractive because it is probably of universal applicability, and the elementary processes which are taken into account are obvious. That model may prove applicable over a wide range of conditions, but the acceleration mechanism is seen most clearly during the breakdown of dense gases by high-voltage pulses with nanosecond rise times, in which case large-factor overvoltages ($\Delta \gg 1$) can be achieved.

In this review we discuss the present state of the nonlocal model for the breakdown of dense gases, and we report research on high-voltage nanosecond discharges in dense gases at high overvoltages. A distinguishing feature of these discharges is that they develop with an intense electron runaway in a dense gaseous medium.

2. HISTORY OF THE QUESTION OF RUNAWAY ELECTRONS IN DENSE GASES. CONDITION FOR RUNAWAY

In 1925 Wilson[41] suggested that a lightning discharge was accompanied by an acceleration of electrons at the front of the leader. Numerous attempts to detect runaway electrons in lightning yielded negative results or were statistically inconclusive. The first reliable results on a detection of this effect in discharges in dense gases were published in 1966 by Frankel *et al*,[42] who by chance detected individual x rays from a helium spark chamber after the passage of a beam of π mesons through it. That paper and some which followed [43,44] reported the detection of x radiation in some specially designed experiments with electric discharges in dense gases. In Refs. 42 and 44, a radiation intensity sufficient to be detected reliably was achieved over 10^4 pulses in discharges in helium at atmospheric density. The radiation dose did not exceed $D_\gamma = 4\cdot 10^{-5}$ R/pulse. Attempts to detect radiation in neon[42] and air[44] were unsuccessful. The excitation of x radiation in those experiments was not a purely gas-discharge effect, since the extremely nonuniform (negative tip)-plane geometry permitted a runaway of field-emission electrons. Using an approximately plane-parallel configuration, Stankevich[43] detected $D_\gamma \approx 4\cdot 10^{-4}$ R/pulse in discharges with high overvoltages in air at atmospheric density. No more than 100- discharges were required for reliable detection. Noggle *et al.*[44] used voltage pulses with a maximum value $U_r^m \approx 300$ kV; the duration of the high-voltage stage of the discharge was $\Delta t_u \approx 80$ ns; and the rise time of the voltage pulse was $\tau_u \approx 10$ ns. The corresponding figures in the experiments by Stankevich were $U_r^m \approx 46$–58 kV, $\Delta t_u \approx 23$ ns, and $\tau_u < 2$ ns. It can be assumed that the radiation was excited during a brief stage of the discharges, lasting less than Δt_u. After Ref. 43 appeared, x radiation and runaway electrons were observed in numerous studies of nanosecond gas discharges in the laboratory.[6,33,45-62] Nanosecond pulses of runaway electrons at relatively low overvoltages ($\Delta \lesssim 1$) were detected during the breakdown of air at atmospheric density by high-voltage pulses in the microsecond range.[63] Some x-ray emission of microsecond duration was detected in the prebreakdown stage in an air-filled decimeter-size gap with an extremely nonuniform geometry.[64] "Nonthermal" penetrating radiation from lightning was detected[65] in 1979; that result was evidence that runaway electrons participate in the dynamics of the lightning. These results serve as convincing experimental confirmation that the electron-runaway mechanism for the breakdown of gas-filled gaps subjected to an overvoltage is of universal applicability.

Stankevich[18] published the first discussion of the condition for electron acceleration during the breakdown of dense gases and the role played by runaway electrons in the dynamics of sparks. Since that discussion was based on the approximation of an elastic energy loss, and the space-charge field $\mathbf{E}_p$ was ignored, the conclusions reached there[18] cannot be used to interpret experiments with discharges in dense gases. In addition, the analytic solutions found for the kinetic equations in Refs. 66 and 67 are also of extremely limited use in application to real experiments. Although Kunhardt and Byszewski[34] worked from a steady-state, symmetric velocity distribution of runaway electrons in weak fields in constructing a mathematical basis for a two-group breakdown model, their specific results were derived from a one-dimensional energy balance equation, as in an earlier paper by Babich and Stankevich,[27] since that approach is successful to some extent in modeling the $\mathbf{E}_p(\mathrm{r})$ profile.

The condition for electron runaway in the intensified electric fields near ionization fronts which are propagating during the breakdown of a dense gas in a uniform external field $\mathbf{E}_0$ (Fig. 1) can be found from the equation of motion

$$\dot{\mathbf{p}} = e\mathbf{E}_f(x, \psi) - L_1(\varepsilon) P \frac{\mathbf{p}}{p}, \tag{2}$$

where $\mathbf{p}$ is the momentum, ψ is the angle between $\mathbf{E}_p$ and $\mathbf{E}_0$, $L_1(\varepsilon) = L_1^{(el)}(\varepsilon) + L_1^{(in)}(\varepsilon)$, and $L_1^{(el)}$ and $L_1^{(in)}$ are respectively the elastic and inelastic energy loss per unit path length at $P = 1$ Torr. In strong fields the relation $L_1^{(el)} \ll L_1^{(in)}$ holds. Below we assume $L_1 \equiv L_1^{(in)}$. Using $\mathbf{p} = (d\mathbf{p}/dx)v\,\overline{\cos\theta}$, where $\overline{\cos\theta} = f(\varepsilon)$ is the average cosine of the angle between $\mathbf{E}_f$ and $\mathbf{p}$, assuming $\mathbf{x}\uparrow\downarrow\mathbf{E}_f$, and multiplying (2) by $\mathbf{p}$, we find a one-dimensional balance equation for the electron energy:[27,33]

$$\frac{d\varepsilon}{dx} = eE_f(x, \psi) - \frac{L_1(\varepsilon)}{\overline{\cos\theta}} P. \tag{3}$$

Electrons are accelerated if the condition $eE_f(x,\psi)/P > L_1(\varepsilon)/\overline{\cos\theta}$ (the runaway condition) holds at the given point in the gap. Figure 2 shows a semiempirical $L_1(\varepsilon)$ dependence for N_2. The maximum value L_1^m in gases is usually near $\varepsilon_{m1} \approx 100$ eV (Table I).[68,69] It can be seen from (3) that only in the case $E_p(x,\psi) = 0$ is the energy ε a function of the scaling parameters Px and E_0/P.

Since the scattering of electrons with $\varepsilon \approx \varepsilon_{m1}$ through large angles is weak,[70] especially in strong fields, the approximation $\overline{\cos\theta} \approx 1$ is quite good. If we incorporate $\overline{\cos\theta}$ we

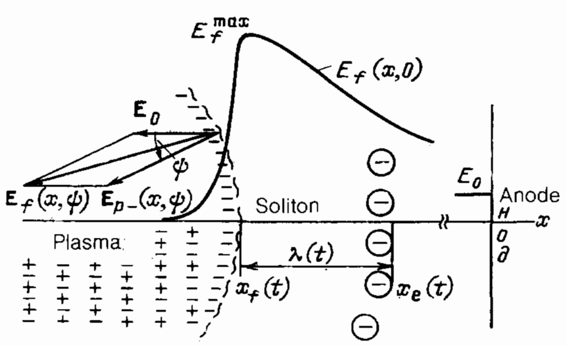

FIG. 1. Diagram of an anode-directed streamer.[34,36]

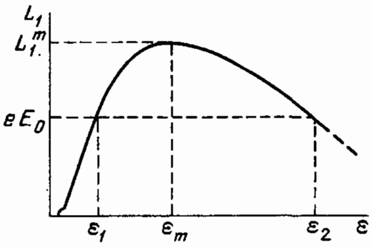

FIG. 2. Electron energy loss per unit path length $L_1(\varepsilon)$, in N_2 at $P = 1$ Torr (Refs. 27 and 68).

find only some broadening of $L_1(\varepsilon)$ in the region $\varepsilon < \varepsilon_{m1}$, with no effect on ε_{m1} or L_1^m. Small-angle multiple scattering, however, increases $L_1^m/\overline{\cos\theta}$.

If $eE/P \gg L_1^m$, then $d\varepsilon/dx \gg 0$, and one can say that beginning at $eE_{cr} = L_1^m P$ there is an electron runaway over the entire energy range which is realized in gas discharges. Values of E_{cr} for $P = 760$ Torr are shown in Table I. If $E < E_{cr}$, then the equation $d\varepsilon/dx = 0$ has two roots: ε_1 and $\varepsilon_2 > \varepsilon_1$ (Fig. 2). For acceleration in fields $E < E_{cr}$, the electrons must be in the energy region $\varepsilon > \varepsilon_2$.

Let us take a more detailed look at electron runaway in a uniform external field $E_0 < E_{cr}$, in which case ε_2 is determined by the equation $E_0 - L_1(\varepsilon)P = 0$. The electrons can acquire an energy ε_2 in part of the gap with $|\mathbf{E}_0 + \mathbf{E}_p| > E_0$. The electron distribution in such regions is very anisotropic and is rich in high-energy electrons. On this basis, Kunhardt and Byszewski[34] adopted the boundary condition $\varepsilon(x = 0) \gtrsim \varepsilon_m$ for Eq. (3) in N_2 at $P = 750$ Torr and with a field $E_0 = 42$ kV/cm. Under such conditions in the avalanche stage, this assumption is not a trivial one, since even at $E_0/P \approx 10^2 - 10^3$ V/(cm·Torr) the relation $T_e \lesssim 10$ eV $\ll \varepsilon_{m1}$ holds in molecular gases. The stage of the breakdown in which the runaway electrons appear depends on E_0/P. These runaways may appear both in the stage of isolated avalanches, in which the parameter E_0/P is quite large, and later, after the avalanche-streamer transition, or as streamers evolve, if the condition $E_0/P \ll (E/P)_{cr}$ holds. Since we have $T_e/\varepsilon_{m1} \ll 1$, the condition $\varepsilon(x = 0) = 0$, without a partitioning of the electrons into two energy groups, is more systematic within the framework of a description of electron runaway by Eq. (3). In addition, it more accurately reflects the transition of some of the electrons into a runaway regime at the front of the ionized region.

As was mentioned in the Introduction, the avalanche-streamer transition occurs over a distance $z_{cr} \approx 100\,\mu$m in a gap with a high overvoltage. The result is the formation of a plasma cloud with a conductivity high enough that it can be modeled by an ideal conductor. In a strong electric field, this cloud becomes polarized. The ionization then develops because of the electrons which detach from the cloud and are

TABLE I.

Gas	ε_{m1}, eV	eV/(cm·Torr)	E_{cr}, kV/cm
He	151	67	51
H_2	50	113	86
O_2	150	356	270
N_2	150	356	270
Xe	100	310	236

TABLE II.

E_0, kV/cm	ε_2, keV	r_0, mm	x_m, mm
100	1.2	6.0	0.36
115	1.1	2.1	0.29
125	1.0	1.0	0.20
150	0.7	0.26	0.09
175	0.55	0.11	0.06

accelerated in the effective range of the space charge. Some of these electrons acquire an energy greater than ε_2 and find it possible to undergo a continuous acceleration all the way to the anode. These electrons effectively emit bremsstrahlung photons, which ionize the gas over the entire electrode gap and knock electrons off the electrodes. As a result, the number of such elementary "accelerators" increases. Kunhardt and Byszewski construe the phrase "runaway electrons" as embracing not only the electrons which reach the anode but also the slower electrons which relax to $v_-(E_0)$ at various points in the gap.[34] The idea of a preacceleration of electrons in a fringing field $\mathbf{E}_f$, with a subsequent "capture" far from this region,[34] underlies the model of contracted channels at relatively low values of $\mathbf{E}_0$. This idea has been used previously to explain the complex spatial structure of nanosecond volume discharges in air at atmospheric pressure at high overvoltages.[33]

Considering a fixed time, putting aside the question of the actual shape of the plasma cloud, and ignoring the effect of the runaway electrons on the magnitude of the polarization, we can use a model of an uncharged spherical conductor of radius r_0 (Ref. 27). We can then write $E_f(x,\psi) = E_0\{1 + 2[r_0/(r_0+x)]^3\}\cos\psi$, where x is reckoned from the surface of the sphere in the direction toward the anode. The runaway condition is approximated by the condition that ε_2 is equal to the maximum value of the solution of Eq. (3) with $\varepsilon(x=0)=0$, $\psi=0$, and $L_1 = L_1^m$. Table II shows values of x_m at which the condition is satisfied, according to calculations for N_2 at $P = 760$ Torr in fields $E_0 > E_{cr}$. The data in Table II give an order-of-magnitude picture of the situation. Numerical calculations based on Eq. (3) are also based on models.[27,34] Alkhazov[71] has numerically solved the kinetic equation for electrons in helium with an unperturbed field $E_0 < E_{cr}$. Isolated runaway electrons were found as a result. Since those calculations "were of a very qualitative nature,"[71] that result is also merely illustrative. Some more-convincing calculations have been carried out by the Monte Carlo method in an unperturbed field.[72] For N_2, a field E_{cr} 1.5 times the value in Table I was found. Although the analytic and numerical studies in Refs. 27, 33, 34, 71, and 72 give only an approximate description of certain aspects of the dynamics of discharges with an overvoltage in dense gases, they do draw an outline of a nonlocal theory which incorporates the complicated interplay of ionization and acceleration processes.

3. BASIC INFORMATION ON THE DISCHARGES

3.1. Spatial shapes. Voltage and current pulses

Apparatus for generating high-voltage pulses, with voltages up to 300 kV, with subnanosecond fronts was developed in the 1960s. That apparatus made it possible to produce current pulses with a rate of rise $\dot{I} \approx 1$–10 TA/s and a maximum value I_m up to several kiloamperes in gas-discharge gaps of width $d \gtrsim 1$ cm at pressures P of the order of tens or hundreds of torr. The duration of the gas-discharge process was no more than 5–10 ns, and the overvoltage in the high-current stage was by a large factor. The basic units of such generators are a step-up pulse transformer and a switch which increases the steepness of the voltage pulse front.[73] Figure 3 shows the voltage pulse from a generator under open-circuit conditions,[61] $U_{gen}(t)$. The maximum value of the pulse is $U_{gen}^m \approx 300$ kV, and the rise time is $\tau_{gen} \lesssim 0.6$ ns.

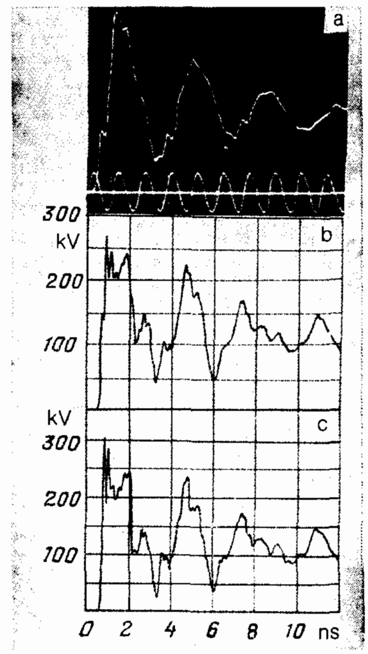

FIG. 3. Voltage pulse from the generator.[61] a–Oscilloscope trace of $U_{gen}(t)$, with an 833-MHz time marker; b–results of numerical simulation of the pulses across a divider; c–the same, across the test gap.

The spatial structure of the emission from a gas-filled gap during a discharge is determined by such factors as the electrode geometry, the gap width d, the pressure and nature of the gas, the inductive and capacitive parameters of the generator, and the breakdown voltage of the steepening switch, U_p. Figure 4 shows photographs of the emission from an air-filled discharge gap for three values of d and for three cathodes; here r_c is the radius of curvature of the working surface of the cathode. The anode was a plane aluminum foil. If the capacitance formed by the switch and the generator chassis is $C_{gen} \approx 50$ pF, and if the inductance of the generator is $L_{gen} \approx 80$ nH, then volume discharges occur at $d \gtrsim 1$ cm. In such discharges, one or several bright plasma regions with an apparent size $l_p \approx 1$ mm $\ll d$ form at the cathode, while the rest of the volume, all the way to the anode, is filled with a relatively faint, diffuse glow. This glow is separated from the plasma beside the cathode and its "corona" by a "dark space."[23,33,58,59] The latter effect is seen particularly clearly at large values of d and r_c. The plasma formations near the cathode are very inhomogeneous. The size of the brightest part of the plasma near the cathode $l_p^{min} \approx 0.3$ for $d = 15$ mm and $r_c = 6$ mm (Ref. 33). As the pressure P is reduced, the size of these plasma formations near the cathode increases, while their brightness decreases. At P of the

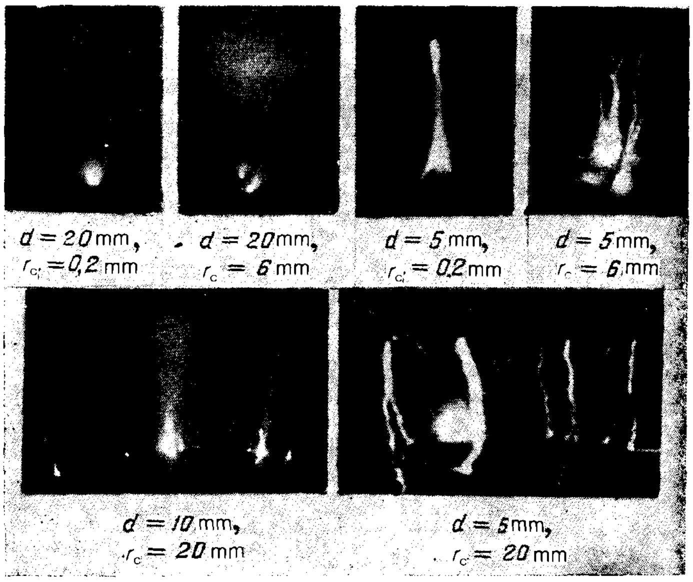

FIG. 4. Emission from an air-filled discharge gap at $P = 760$ Torr and $U^{\rm m}_{\rm gen} \approx 200$ kV (Refs. 23, 33, 58, and 59).

order of tens of torr, a broad channel, several millimeters in diameter, forms. At $P \lesssim 0.1$ torr, one does not observe discharge phenomena with smooth electrodes having an extended working surface; i.e., there is no glow, current, or x-ray emission. If the cathode is sharp or artificially roughened, however, plasma regions considerably smaller than those at $P = 760$ torr form on the cathode surface, and a conduction current and x radiation are detected. In Ref. 45, the volume glow was also separated from the cathode by a dark space at $P = 30$ torr in a plane-parallel geometry.

If d is reduced at atmospheric pressure, a bright contracted channel begins to grow out of the plasma beside the cathode toward the anode. Beginning at $d \approx 1$ cm, this channel completely bridges the gap; i.e., breakdown according to the conventional understanding of the word occurs. One does not detect a visually observable diffuse sheath around the channel. The number of channels or of plasma regions beside the cathode increases with increasing uniformity of the field: At $r_{\rm c} \gtrsim 6$ mm, one usually observes several channels or plasma regions. In gaps with an extremely nonuniform geometry, either a single channel or a single plasma region forms.

The mean value of d which separates the regions in which the two forms of the discharge exist depends on the resonant frequency of the generator, ω_0: As $C_{\rm gen}$ and/or $L_{\rm gen}$ is increased, the discharge contracts at a progressively larger value of d, in accordance with an increase in the length of the current pulse, Δt_I. Since an open-circuit regime prevails at sufficiently large values of d, there is an interval of d values in which a volume discharge forms. This interval shrinks as ω_0 is reduced, and at certain sufficiently small value of ω_0 the discharge always contracts.

On the basis of their formation conditions and spatial structure, nanosecond volume discharges at high overvoltages can apparently be regarded as high-voltage pulsed coronas or an incomplete breakdown in the conventional understanding of the word.

An overvoltage by a large factor leads to ionization propagation velocities which are comparable to the velocity of light, and current pulses with a rate of increase $\dot{I} \approx 1$–10 TA/s form.[33,54,59,74] On the oscilloscope trace in Fig. 5, the rise time of the current pulse in the volume discharge is $\tau_I > 0.5$ ns. The maximum value of the current is $I_{\rm m} \approx 1.5$ kA, while the average current density in the plasma beside the cathode is $j_{\rm p} \sim I_{\rm m}/l_{\rm p}^2 \approx 100$ kA/cm^2. As d decreases in the transition to the contracted form of the discharge, the conductivity and thus $I_{\rm m}$ increase, while the current and the voltage become oscillatory (Fig. 6).

An important characteristic of the rate of development of the ionization processes is the delay of the breakdown

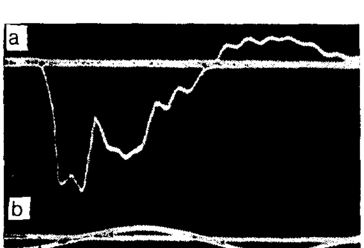

FIG. 5. a–Oscilloscope trace of the current in air at $U^{\rm m}_{\rm gen} = 200$ kV, $P = 760$ Torr, and $d = 15$ mm with a sharp conical cathode ($r_{\rm c} = 200$ μm); b–100-MHz time marker.

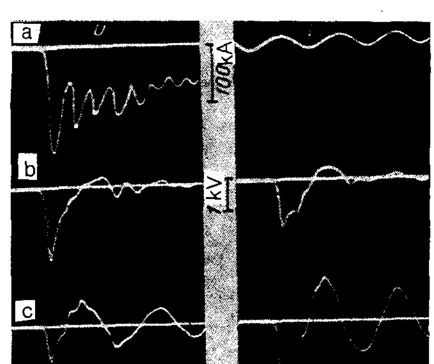

FIG. 6. Oscilloscope traces of the voltage U and the current I in air at $P = 760$ Torr with $U^{\rm m}_{\rm gen} = 200$ kV. a–The $U_{\rm gen}(t)$ pulse, with a 100-MHz time marker; b–d = 15 mm; c–d = 5 mm (Refs. 48 and 74).

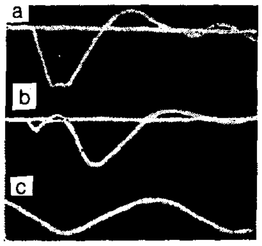

FIG. 7. Oscilloscope traces of the current in air at $P = 760$ Torr, $U^{m}_{gen} = 150$ kV, and $d = 1$ cm. a–Sharp conical cathode ($r_c = 200\ \mu$m); b–hemispherical cathode ($r_c = 2$ cm); c–100-MHz time marker.

with respect to the time at which the voltage pulse is applied, t_d. If $d \lesssim 1.5$ cm and $U^{m}_{gen} \gtrsim 180$ kV, a large conduction current appears at the front of the voltage pulse itself in air at atmospheric pressure, regardless of the cathode geometry, and U^{m}_{gen} is not reached (Fig. 6). In other words, we have $t_d < \tau_u < \tau_{gen} \lesssim 0.6$ ns, where τ_u is the rise time of the voltage pulse across the discharge gap. The ionization propagation velocity, $v_f > d/t_d > d/\tau_{gen} > 2.5 \cdot 10^9$ cm/s, is thus greater than the streamer propagation velocity by more than an order of magnitude at relatively low overvoltages.[11,12] It should be kept in mind that until the voltage reaches the static breakdown voltage U_s there will be no discharge phenomena in the gap; in this sense, even d/τ_u is a lower estimate of v_f.

If $U^{m}_{gen} < 180$ kV, it is possible to detect t_d in the case of a relatively uniform field. Figure 7 shows oscilloscope traces of the current in geometric configurations which differ greatly in the value of the field near the cathode, E_c. On oscilloscope trace b at the left we see a bias current I_b (the current which is charging the capacitance of the electrode gap). This bias current is not found on trace a. The absence of I_b implies $t_d \ll \tau_u$. For a cathode with $r_c = 2$ cm we have $t_d \approx 2$ ns. The value of E_c is determined by the current rise time: At $r_c = 200\ \mu$m we have $\tau_I \approx 0.8$ ns, while at $r_c = 2$ cm we have $\tau_I \approx 1.2$ ns.

The delay t_d increases with decreasing pressure P (Fig. 8).[59] In other words, a decrease in P is equivalent to a decrease in E_c. The meaning here is that at a fixed value of d the ionization rate is determined by the values of E and P separately, not by their ratio E/P, as it would be in a local model of breakdown.

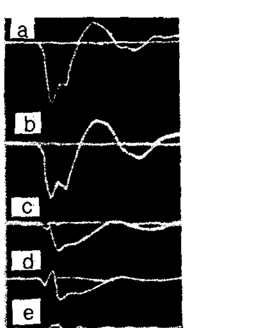

FIG. 8. Oscilloscope traces of the current in air at $U^{m}_{gen} = 270$ kV, $d = 15$ mm, and $r_c = 6$ mm. a–$P = 760$ Torr; b–470 Torr; c–40 Torr; d–15 Torr; e–capacitive current for an oil-filled gap; f–100-MHz time marker.[59]

3.2. Spectra and space-time evolution of the emission from the plasma of a volume gas discharge

The pronounced variations in space and time in the discharge process and the strong external electric field E_0 seriously limit diagnostics of the parameters of the discharge plasma. The most serious limitations are on the accuracy with which the "temperature" and the degree of ionization can be determined. The optical emission from volume discharges in air at atmospheric pressure was studied in Refs. 23, 58, and 59. In the spectra of the plasma near the cathode, a continuum with a characteristic maximum was found; in addition, bands of the second positive system of the N_2 molecule, an NII line, an HI line (656.285 nm, and lines of atoms of the cathode material were found. In the case of a stainless steel cathode, more then 100 lines of FeII and 17 of CrII were observed. No lines of ions with a higher ionization multiplicity were observed. In the case of a cathode made of a VNM alloy (W-Ni-Cu), only four easily excited WI lines were detected. The temperature of the plasma near the cathode was estimated from a Wien's-law distribution of the continuum to be $T \approx 0.5$–0.6 eV. The electron temperature in the plasma near the cathode was found by the Ornstein method to be $T \approx 1.8$ eV. The electron density $n_e \approx 2 \cdot 10^{17}$ cm^{-3} corresponds to a degree of ionization $i \approx 10^{-2}$ and agrees with the results of Ref. 75. The time scale of the relaxation to an equilibrium electron distribution, $\tau_{ee}(T_e, n_e) \approx 1$ ps, is far shorter than the time scales of the voltage and current pulses.

In the diffuse glow of the main volume, only bands of the second positive system of N_2 were detected. These bands were the same as those detected near the cathode, where they are emitted by a halo around the hotter plasma core. The degree of ionization of the main volume was $i < 10^{-5}$.

The emission in the N_2 bands and the NII lines in the plasma beside the cathode begins 1–2 ns before the continuum and the metal lines appear.[23] This result contradicts the data of Ref. 76, where a study was made of a nanosecond volume discharge in air at $P = 760$ Torr, $d = 230\ \mu$m, $U^{m}_{gen} \approx 7$ kV, and $I_m \approx 30$ A. This result corresponds to the physics of the process, since the explosion of microscopic protuberances on the cathode surface with a delay $t_{pre} \approx 1$ ns requires the flow, for a time t_{pre}, of a prebreakdown thermionic-field-emission current of huge density,[4] $j_{cr} \approx \{[4 \cdot 10^9\ A^2 s/(cm^4)] \cdot t_{pre}^{-1}\}^{1/2} \approx 10^9$ A/cm^2. A single emission electron would be sufficient to initiate an electron avalanche in a gap with a high overvoltage, on the other hand, and emission from the gas should precede emission from the cathode explosion products.

The duration of the emission in the N_2 bands and in all the lines is negligibly greater than the duration of the current pulse, Δt_I. The recombining plasma beside the cathode emits a continuum for $\sim 1\ \mu$s.

The time evolution of the optical emission is illustrated by the photochronogram in Fig. 9 (Ref. 23). The plasma near the cathode is separated by a dark space from the region of the diffuse glow in the volume. The duration of the latter is essentially the same as the duration of the current, Δt_I. The plasma beside the cathode expands for a time Δt_I, and its emission intensities. Emission from decaying plasma is then detected for $\sim 1\ \mu$s. The average plasma expansion velocity over Δt_I is $\sim 3 \cdot 10^7$ cm/s. The propagation velocity of the diffuse glow in the volume and of the faint glow near the cathode, which precedes the formation of the bright plasma,

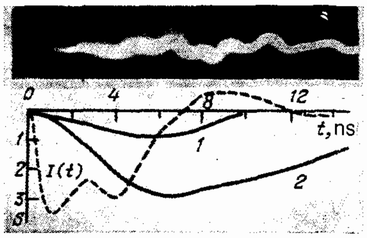

FIG. 9. Photochronogram of the emission of the volume discharge in air at $P = 760$ Torr, $U_{\text{gen}}^{\text{m}} = 270$ kV, $d = 15$ mm, and $r_c = 3$ mm (Ref. 23). Here S is the blackening density of the film caused by (1) the diffuse glow and (2) the emission from the plasma beside the cathode; I(t) is an oscilloscope trace of the current.

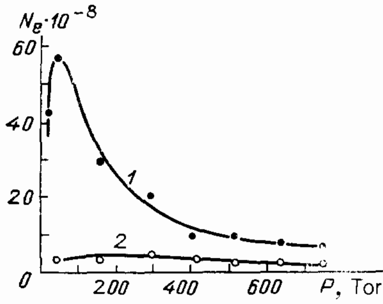

FIG. 10. Curves of Ne(P). *1*–Filter of 5 mg/cm² ($\varepsilon \gtrsim 40$ keV); *2*–53 mg/cm² ($\varepsilon \gtrsim 200$ keV) ($U_{\text{gen}}^{\text{m}} = 270$ kV, $d = 15$ mm, $r_c = 6$ mm).[50]

is very high: From the photochronogram we estimate a lower limit of $2 \cdot 10^9$ cm/s on this velocity. This estimate corresponds to the estimate of v_f above. The propagation velocity of the volume emission thus appears to be substantially higher than $d/\tau_I \approx (1.5\ \text{cm})/(0.5\ \text{ns}) = 3 \cdot 10^9$ cm/s, since the emission appears at the same time as the conduction current. Such a high propagation velocity of ionization fronts requires a special explanation.

According to a densitometer study of the photochronogram, the blackening S caused by the emission from the cathode region and that caused by the volume emission agree during the first 0.5 ns. Over the same time ($\tau_I < 0.5$ ns), the current rises to its maximum value. As was mentioned above, during this time interval the cathode region emits only in the N_2 bands and the NII lines. Immediately after the current reaches its maximum, the lines of the metal and the intense continuum appear, while the emission from the plasma beside the cathode intensifies sharply.

It can be concluded that over a time shorter than τ_I a faintly glowing streamer, separated from the rest of the volume by a dark space in Fig. 9, develops near the cathode. Since the thickness of this streamer is much smaller than the transverse dimension of the rest of the emitting region in the discharge gap, the fact that the blackening levels are the same means that the energy emitted by a unit surface area of the streamer is greater than that emitted by a unit surface area of the volume filled by the diffuse glow.

The slight heating of the plasma of a nanosecond volume gas discharge at high overvoltages, the low degree of ionization of this plasma, and the absence of lines of highly ionized atoms at a current density $j_p \approx 100$ kA/cm² and a high voltage (on the one hand) and the fact that the velocity of the ionization fronts is comparable to the velocity of light, the formidable rate of increase of the current ($\dot{I} \approx 1$–10 TA/s), and the spatial structure of the emission (on the other) can be interpreted in terms of runaway electrons in a dense gaseous medium (§6).

4. RUNAWAY ELECTRONS

4.1. Number and energy distributions of the runaway electrons

The first experiments with high-voltage nanosecond discharges in dense gases at high overvoltages revealed a penetrating radiation, intense enough to cause a pronounced blackening of RT-1 x-ray film behind a window in the discharge chamber.[48,50,51] A comparison of experimental data with calculations on the absorption of electrons and x radiation in filters with various value of Z led to the unambiguous conclusion that the radiation detected in Refs. 48, 50, and 51 consisted of runaway electrons, in contrast with that in Refs. 42–45 and 49. The number of these electrons beyond the chamber window varied with the particular conditions (the pressure P, the type of gas, U_p, the cathode geometry, and d) over the range $N_e \approx 10^8 - 10^{12}$ e⁻/pulse $\approx 2(10^{-6} - 10^{-2})Q_0/e$ (Ref. 50), where Q_0 is the initial charge on the storage capacitance of the generator, C_{gen}. The gases which were studied at $P = 760$ Torr can be arranged in order of decreasing N_e: He, Ne, $H_2(D_2)$, Ar, Xe, SF_6. The $N_e(P)$ dependence is shown in Fig. 10. The decrease in N_e at $P \lesssim 50$ Torr on curve 1 is a consequence of a decrease in the rate of ionizing collisions of electrons. Discharges did not develop in experiments with smooth cathodes at $P \lesssim 0.1$ Torr; i.e., the dynamics of the breakdown is determined by electron breeding in the gas. In gaps with sharp cathodes, emission processes also become important, and the maximum on the $N_e(P)$ curve shifts into the region $P \lesssim 0.1$ Torr. According to curve 2, the distribution depends only weakly on P in the high-energy region (see the discussion below of the generation of electrons of "anomalous energy"). The discharges in helium are distinguished by an increase in the high-energy part of the distribution (compare Figs. 12c and 12e) and by a large number of runaway electrons. By way of comparison, with a filter of 5 mg/cm² in air we have $N_e \approx 10^9$ e⁻/pulse at $P \approx 760$ Torr, and the maximum value $N_e^{\text{m}} \approx 6 \cdot 10^9$ e⁻/pulse is reached in the interval 50–100 Torr (Fig. 10). In helium, we have $N_e^{\text{m}} \approx 5 \cdot 10^{11}$ e⁻/pulse at

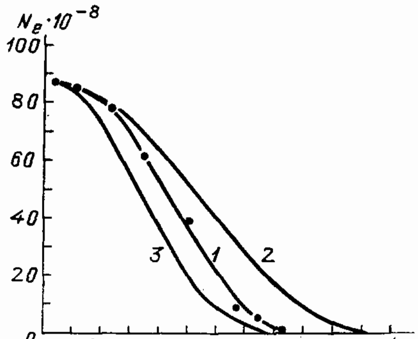

FIG. 11. Curves of the absorption of electrons in Al. *1*–High-voltage nanosecond discharge ($U_{\text{gen}}^{\text{m}} = 270$ kV, air, $P = 760$ Torr, $d = 15$ mm, $r_c = 6$ mm; Ref. 51); *2*,*3*–data of Ref. 77 for $\varepsilon = 336$ keV and $\varepsilon = 250$ keV.

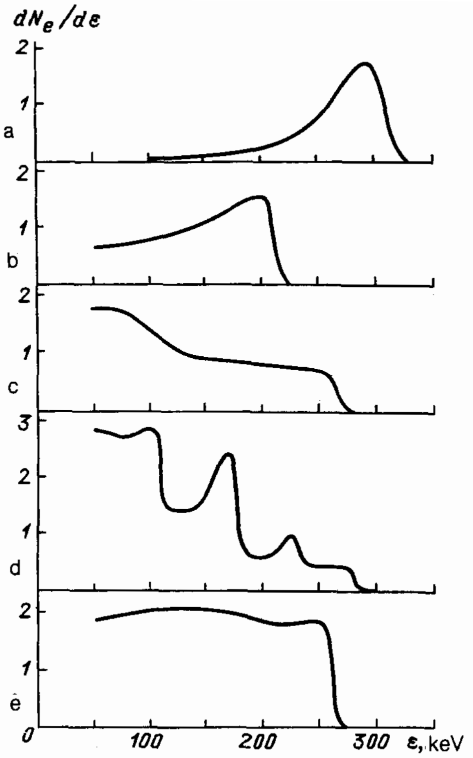

FIG. 12. Energy distributions of runaway electrons.[61] Air: a–760 Torr, 500 pulses; b–70 Torr, 300 pulses; c–22 Torr, 100 pulses; d–0.2 Torr, 5 pulses. Helium: e–22 Torr, 10 pulses ($U_{gen} = 270$ kV, $d = 2$ cm, $r_c = 200$ μm, grid anode).

$P \approx 22$ Torr. Rough estimates of the energy of the runaway electrons were found by plotting curves of the absorption in metal filters.[50,51] The nature of the curves usually corresponds top a broad energy distribution, but at pressures of the order of hundreds of Torr it is typical to find curves which are characteristic of monoenergetic electrons, e.g., curve 1 in Fig. 11, which corresponds to[51] $\varepsilon \approx 270$ keV $> eU_m$. The energy distributions of the runaway electrons were found by a magnetic spectroscopy method.[61] The results for one geometric configuration are shown in Fig. 12. The filtering of the electrons before they enter the vacuum chamber of the spectrometer, with 6 mg/cm^2, corresponds to the range of electrons with an energy $\varepsilon \approx 50$ keV. At air pressures $P \gtrsim 200$ Torr, the electron energy distribution has a well-defined maximum, whose position moves up the energy scale as P is increased. The measured width of the distribution, $2\Delta\varepsilon \approx 60$ keV, is essentially independent of P over the range 200–760 Torr. Since the results of these measurements depend on the scatter in the values of U_p and U_m, on the width of the slit diaphragms of the collimator, and also on the scattering in the chamber window, the intrinsic spectral width is $2\Delta\varepsilon < 60$ kev. This figure agrees with absorption curves which are characteristic of monoenergetic electrons (Fig. 11). At $P < 200$ Torr the maximum is spread out by the appearance of a large number of slow electrons (Fig. 12, b and c). As P is reduced, the maximum energy ε_{max} initially decreases, and then it increases again, in accordance with the $U_m(P)$ curve, reaching $\varepsilon_{max} \approx eU_{gen}^m \approx 270$ keV at $P \approx 22$ Torr. At $P \lesssim 1$ Torr, the distribution of runaway electrons becomes a line spectrum (Fig. 12d), reflecting the structure of $U_{gen}(t)$ (Fig. 3). The value $\varepsilon_{max} \approx eU_{gen}^m \approx 270$ keV persists.

4.2. Generation of "anomalous-energy" electrons

It follows from the curves of the absorption of electrons and of the energy distributions that there is a generation of electrons of "anomalous energy," with $\varepsilon > eU_m$, in air at sufficiently high pressures.[23,33,50,51,54,60–62] Table III shows value of U_m and of the electron energy at the spectral peak, ε_m, for several values of d at $P = 760$ Torr. For $d \gtrsim 1$ cm we have $\varepsilon_m - eU_m = 100 - 110$ keV, while for small values of d this different is much smaller. We recall that at $d \gtrsim 1$ cm the discharge is a volume discharge, while at $d \lesssim 1$ cm a contracted channel forms.

The electron distribution is strongly influenced by the curvature of the cathode, which affects not only the value of U_m but also the distribution and magnitude of the field in the gap. In air at $P = 760$ Torr and $d = 2$ cm, the maximum energy $\varepsilon_m \approx 320$ keV was found in experiments with a conical cathode of a VNM (W-Ni-Cu) alloy with a vertex angle $2\beta = 60°$ and $r_{cr} \approx 3$ mm. When a zince cathode is used in the same geometry, the value $\varepsilon_m \approx 260$ keV is found: The value of U_m and thus that of ε_m are affected by the emission and thermal properties of the cathode.

Convincing evidence for the generation of anomalous-energy electrons emerged from experiments, proposed by G. A. Askar'yan, in which retarding voltage pulses identical to the accelerating pulses were used.[61] In these experiments, a pulse of positive polarity was applied to a high-voltage grid electrode. A conical cathode was installed on the inner surface of a grounded cylindrical chamber, at a distance $d = 2$ cm from the anode grid. The runaway electrons passed through the anode into the region of retarding field, where they traversed a potential difference $\Delta\varphi_T = -U(t)$. A film cassette with RT-1 film was positioned diametrically opposite the cathode, 2 cm from the anode. Wedges were placed in front of this film for estimates of ε. Runaway electrons with $\varepsilon \leqslant eU_m$ did not reach the film, since they lost energy in the gas and the cassette. At $P = 760$ Torr, the energy of the electrons traversing $\Delta\varphi_T$ was 90 keV.

Experiments were carried out[54] in air at $P = 760$ Torr in order to study this effect. It was found that regardless of whether U_m increases or decreases in a given series of experiments the number of anomalous-energy electrons, N_e, is essentially independent of I_m. The value of ε_m varies slightly in the same directional as U_m. The number N_e increases slightly with increasing Q_0: by 20% as Q_0 is increased by a factor of 2.5. The value of ε_m remains essentially constant. Experiments with a variety of steepening switches revealed that the generation of anomalous-energy electrons becomes more prominent as the front of the voltage pulse becomes steeper.

The distributions of the runaway electrons in discharges in air at atmospheric density thus contain a component whose energy is about 100 keV above the value of eU_m. Since this effect depends only weakly on I_m and Q_0, and the

TABLE III.

d, cm	0,5	1	2	3,5
U_m, В	130	150	190	210
ε_m, кэВ	180	260	290	320

anomalous-energy electrons are concentrated in a narrow energy interval ($2\Delta\varepsilon \ll \varepsilon_m$), these electrons do not belong to tails on the energy distribution of the electrons of the discharge plasma.

4.3. Space-time characteristics

In order to identify the mechanism by which the runaway electrons participate in the dynamics of the discharges, it is important to know the space-time characteristics of these electrons: the region in which they are generated, their divergence, the pulse length Δt_e, and the time at which the generation begins with respect to the time at which the voltage pulse is applied to the gap. In an effort to localize the region in which the runaway electrons are generated, a study was made of the spatial structure of the cross section of the fluxes of these electrons beyond the anode. Figure 13a shows an image of the runaway-electron flux for discharges in He at $P = 22$ Torr. The filter here was 45 mg/cm^2 ($\varepsilon \gtrsim 200$ keV). The image corresponds to a grid of notches on the working surface of the cathode. The source of the stream of runaway electrons is thus the cathode or the plasma beside the cathode, which forms near the edges of the notches. The spatial distribution of the runaway electrons is strongly influenced by scattering by molecules in air at $P = 760$ Torr. In experiments with a sharp conical cathode, however, it was found that the width of the runaway-electron beam clearly depends on d: For $d = 5$ mm, the beam width is $\phi_e = 5$–6 mm, while for $d = 15$ mm it is $\phi_e = 3$ cm (Fig 13, b and c). If several channels form in the discharge—this is a typical observation for cathodes with an extended working surface—the number of channels is equal to the number of beams in the electron flux beyond the anode. This circumstance is particularly obvious at $d \lesssim 5$ mm, at which the width of the beams is quite small: $\phi_e \approx 1$ mm (Fig. 13c). The structure of the flux corresponds to the distribution of emitting centers on the cathode. The source of the runaway electrons in air at $P = 760$ Torr is thus the cathode region.

Measurements of the temporal characteristics of the pulses of runaway electrons are of particular interest for learning about the electron acceleration mechanism and for determining the role played by the runaway electrons in the dynamics of discharges. The intensity of the runaway electrons was not sufficient for direct time-resolved measurements in all the regimes of importance here. Figure 14 shows oscilloscope traces of the pulses of runaway electrons in helium (the spectrum in Fig. 12) obtained through direct detection with a Faraday cup, for two filters. The rise time of the pulse of runaway electrons is $\tau_e < 0.5$ ns. The length of the pulse at the level of 0.1 of the maximum value is $\Delta t_e = 2$ ns for $\varepsilon \gtrsim 50$ keV or $\Delta t_e \approx 1.3$ ns for $\varepsilon \gtrsim 100$ keV. In air at P of the order of hundreds of Torr, the pulse of anomalous-energy electrons was measured with time resolution by a method involving the conversion of the electron energy into light with the help of some fast plastic scintillators[61,78] (Fig. 14d). The pulse rise time was $\tau_e < 0.4$ ns, and the length of the pulse at half-maximum was $\Delta t_e \approx 0.5$ ns (allowance is being made here for the exponential afterglow of the SPS-B-12 plastic). As the air pressure is reduced, Δt_e increases, and at $P \approx 10$ Torr it turns out to be approximately equal to the half-width of the first maximum on the oscilloscope trace of $U^m_{gen}(t)$.

In order to reach an understanding of the role played by the acceleration processes in the physics of discharges, it is particularly important to identify the beginning of the generation of accelerated electrons. Under conditions such that it is not possible to detect the retardation of the current with respect to the time at which the voltage pulse is applied (Figs. 6–8), the anomalous-energy electrons are detected at the front of the voltage pulse $U(t)$. It would be natural to assume, however, that the generation of these electrons occurs not during the rise of $U(t)$ but slightly later: on the current front. To prove this assumption, it is necessary to delay the emission from the cathode and to retard the onset

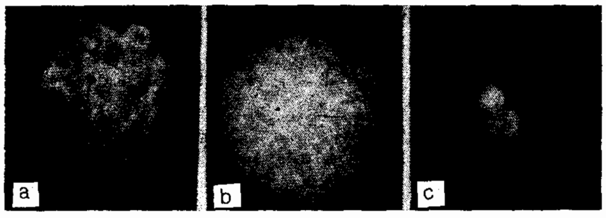

FIG. 13. Images of electron fluxes beyond the anode[48,50] [He, $P = 760$ Torr, $d = 10$ mm (*a*); air, $P = 760$ Torr, $d = 15$ mm (b) or $d = 5$ mm (c)]. $U^m_{gen} = 270$ kV.

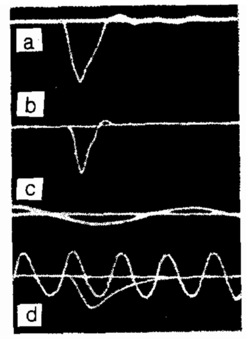

FIG. 14. Oscilloscope traces of pulses of runaway electrons in He at $P = 22$ Torr. a–Filter of 7 mg/cm^2 ($\varepsilon \gtrsim 50$ keV); b–20 mg/cm^2 ($\varepsilon \gtrsim 100$ keV); c–10-MHz time marker; d–oscilloscope trace of the emission from SPS-B12 plastic excited by a pulse of anomalous-energy electrons during discharges in air ($P = 760$ Torr). The time marker is 833 MHz; $U^m_{gen} = 270$ kV; $d = 2$ cm, $r_c = 200\,\mu$m (Refs. 61 and 78).

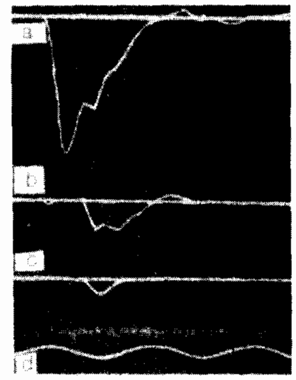

FIG. 15. Oscilloscope traces of the pulses of the voltage U(a) and the current I(b) in a discharge gap and of the pulse of runaway electrons (c). $U^m_{gen} = 240$ kV, air, $P = 760$ Torr, $d = 1$ cm, $r_c = 6$ mm. d–100-MHz time marker.[33]

of ionization processes, so that the current delay t_d will be substantially greater than τ_u. here is sufficient to construct a barrier discharge.[33] Figure 15 shows oscilloscope traces of $U(t)$, $I(t)$, and the pulse of anomalous-energy electrons in this regime. The small peak at the left is the bias current. A maximum value $t_d \approx 4$ was found. The point at which anomalous-energy electrons start to appear coincides with the beginning of the conduction current. In discharges with a smooth cathode at a reduced pressure in helium or air, in which cases significant values of t_d are observed, the beginning of the pulse of runaway electrons also coincides with the beginning of the conduction current. Since the value $\Delta t_e \approx 0.5$ ns does not exceed τ_I, it is logical to suggest that the anomalous-energy electrons are generated during the rise of the conduction current and that this generation comes to a halt no later than the time at which the current reaches its maximum value.

4.4. Runaway electrons during the breakdown of air by high-voltage microsecond-range pulses

Since the runaway electrons have a high ionizing capability and should strongly influence the dynamics of discharges, experiments were undertaken to detect these electrons during the breakdown of air at atmospheric density by microsecond voltage pulses.[63] In these experiments, the values of Δ were relatively low, corresponding to the classical streamer model of Raether. For this purpose, the steepening switch was removed from the voltage pulse generator. The test gap had a conical cathode with $r_c \approx 3$ mm, a grid anode, and $d = 0.5$–3 cm. The maximum value of the pulsed voltage across the gap varied considerably ($U_m = 60$–80 kV at $d = 2$ cm), but it stabilized at $U_m = 50$ kV in the case of exposure to UV light. Regardless of whether this exposure was made, the contracted channel formed in any configuration of the gap. The maximum value of the current pulse was $I_m \approx 200$ A at $\tau_I \approx 4$ ns. Exposure to UV light increased τ_I to 8 ns. When RT-1 film was positioned 3 cm behind the anode, it was irradiated only in experiments without exposure to UV light, with $\Delta \approx 0.6$. On the basis of the weak dependence of the blackening on the value of Z of the absorber, it was concluded that electrons were detected. The broadening of the beam was proportional to d; i.e., the source of the runaway electrons was the cathode region. The number of these electrons was $N_e \approx 10^7$ at $Q_0/e \approx 2 \cdot 10^{13}$, and their energy was $\varepsilon \approx 70$ keV $\approx eU_m$. The duration of the pulse of runaway electrons, $\Delta t_e \approx 3.5$ ns, was equal to the time resolution of the measurement system. The runaway electrons were detected at the front of the conduction-current pulse. In the case of exposure to UV light, N_e and ε should decrease substantially; the absence of blackening may mean nothing more than that the runaway electrons are absorbed in the medium before they reach the RT-1 film.

The generation of runaway electrons at small values of Δ is evidence that some mechanism other than the conventional streamer mechanism is responsible for the breakdown of the dense gases. At any rate, the second of the three streamer-model ideas listed in the Introduction must be seriously modified. To the extent to which the discharges studied in Ref. 63 model lines lightning, the experiments, along with Whitmire's results,[65] can serve as confirmation of the hypothesis that lightning is capable of generating runaway electrons.

TABLE IV.

δ, μm	$D_\gamma^{(э)}$, Р/имп	$D_\gamma^{(T)}$, R/pulse
0	7,8	7,4
270	3,6	3,2
540	2,3	2,5

5. EMISSION OF x RADIATION

There is no difficulty in studying the x-ray pulses in discharges in gas-filled gaps subjected to a high overvoltage, because the emission is quite intense.[50–52] Table IV shows measurements of the x-radiation dose $D_\gamma^{(\text{exp})}$ under the conditions for which the runaway-electron absorption curve in Fig. 11 was recorded. The electrons were absorbed in a layer of polyethylene (2 mm thick) and in an aluminum-foil anode (8 μm thick). An aluminum layer of thickness δ was placed between the polyethylene and the dosimeter. The energy of the x rays was found from the layer thickness ($\delta_{1/2}$) which resulted in a 50% attenuation to be $\bar{\varepsilon}_\gamma \approx 14$ keV.

Kremnev and Kurbatov[49] carried out an experimental and theoretical study of the behavior of the x-ray energy W_γ as a function of E_0/P in nanosecond discharges in dense gases. Those calculations used the drift approximation for the current, and $\mathbf{E}_p$ and the runaway electrons were ignored. Gurevich's expressions[66] for the steady-state flux of runaway electrons in weak fields were used, and Kramers' approximate formula was used for the emission intensity. The value of ε_γ was related to the electron energy ε by $\varepsilon_\gamma = 2\varepsilon/3$, but that step was a result of a misunderstanding: The quantity $\lambda_\gamma = 3hc/2\varepsilon$ corresponds to the maximum of the wavelength distribution of the emission intensity for a thin target. the calculated and experimental values of $W_\gamma(E_0/P)$ turned out to differ by a factor of 2 or 3 (Ref. 49).

If the energy distributions of the runaway electrons and their flux $\Phi_e = N_e/S_e$ are measured directly, one can compare the experimental and theoretical characteristics of the x-ray emission without appealing to any hypothesis regarding the conductivity mechanism and without calculating Φ_e. By using the Sommerfeld formula for the bremsstrahlung cross section, the Bethe formula for the inelastic energy loss of the electrons, and the assumption that the absorption of radiation energy between the point of emission and the detector is exponential, one can calculate the spectra of the photons (N_{ε_γ}), the intensity I_{ε_γ} and the dose D_{ε_γ} at the exist from a thick layered target. One can then calculate the total dose[51]

$$D_\gamma = \int_0^{\varepsilon_0} D_{\varepsilon_\gamma} \, d\varepsilon_\gamma,$$

where ε_0 is the initial energy of the electrons incident on the target. Table IV shows results calculated for D_γ^{theor} for anomalous-energy electrons ($\varepsilon_0 = \varepsilon_m$). We see that there is an agreement, $D_\gamma^{\text{exp}} \approx D_\gamma^{\text{theor}}$, and the value of $\bar{\varepsilon}_\gamma$ found from $\delta_{1/2}$ for D_γ^{theor} is close to 14 keV. The x radiation detected in air at $P = 760$ Torr is thus the bremsstrahlung of anomalous-energy electrons in the anode.[51] If we use the relation $\varepsilon_\gamma = 2\varepsilon_m/3$, we find a line with $\varepsilon_\gamma \approx 200$ keV instead of a spectrum of photons, and this conclusion could not be correct. Note that the value of $\bar{\varepsilon}_\gamma$ found from $\delta_{1/2}$ depends only

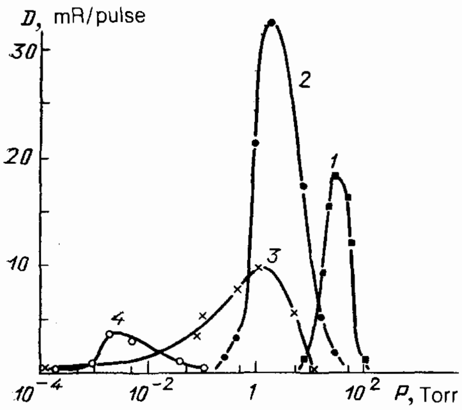

FIG. 16. Dose of x radiation as a function of the pressure.[52] 1–Chamber 1, He; 2–chamber 1, air; 3–chamber 2, air ($U^{m}_{gen} = 250$ kV, $\tau_{gen} \lesssim 0.6$ ns); 4–chamber 2, air ($U_m = 110$ kV, $\tau_{gen} = 1$ μs).

weakly on ε_0, and its relatively small value (~ 10 keV; Refs. 42–44) could not characterize the energy of runaway electrons in dense gases. Since the number of spectrum of the runaway electrons depend on the pressure, the x-ray dose also depends on the gas pressure. The dependence $D_\gamma(P)$ was studied in Ref. 52 for discharges in approximately uniform fields, so there was no explosive electron emission. These measurements were carried out in two chambers. In chamber 1, the cathode was a sheet of aluminum foil with a thickness $\delta = 15\,\mu$m, while the anode was a steel hemisphere 4 cm in diameter. In chamber 2, the thickness of the cathode was $\delta = 8\,\mu$m, and the anode was a cone ($2\beta = 60°$) with $r_c \approx 3$ mm, made of a VNM (W-Ni-Cu) alloy. The gap length was $d = 15$ mm. Pulses with a rise time $\tau_{gen} < 0.6$ ns or $\tau_{gen} \approx 1$ μs were applied to the gap. The emission was detected 3.5 cm behind the cathode. The results are shown in Fig. 16. The position (P_m) of the maximum value of the dose D^{m}_{γ} is determined primarily by the type of gas and the voltage pulse. For microsecond pulses, the result $P_m \approx 4\cdot 10^{-3}$ Torr was found (curve 4). The shortening of τ_{gen} leads to an upward shift of P_m (curves 1–3): Values $P_m \approx 1$–3 Torr were found for air, and $P_m \approx 20$ Torr was found for helium.

For the given electrode configuration, D_γ in vacuum is much smaller than D^{m}_{γ}; i.e., the runaway electrons are generated as a result of volume ionization processes. At large values of P, at which the x-ray intensity is low, the discharge develops in the form of bright contracted channels. As P is reduced, the channel width increases, and near P_m there is a spatially uniform discharge. These results agree with those of Ref. 44, where the channel width decreased with increasing atomic number of the gas [and thus with increasing electron energy loss $L_1(\varepsilon)$]. These results can serve as evidence

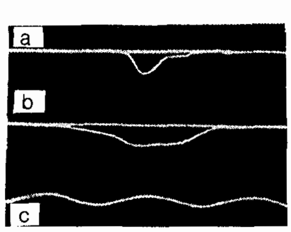

FIG. 17. Oscilloscope traces of the pulses of x radiation in air near P_m. a–$\tau_{gen} \lesssim 0.6$ ns; b–$\tau_{gen} = 1$ μs; c–100-MHz time marker.[78]

TABLE V.

ε_0, keV	5	10	15	25	100	250
$I^{(air)}_{\gamma}/I^{(Al)}_{\gamma}$	88	22	10	4	1	0,04

that a volume form of the discharge is consistent with acceleration processes.

Figure 17 shows oscilloscope traces of the x-ray pulses in air near P_m. The pulse length at half-maximum is $\Delta t_\gamma \approx 2.6$ ns at $\tau_{gen} \lesssim 0.6$ ns and $\Delta t_\gamma \approx 8$ ns at $\tau_{gen} \approx 1$ μs.

We thus see that in discharges in dense gases it is possible to produce substantial doses of x radiation. This radiation therefore not only is an important source of information about the processes which occur in the discharge gap but can also be utilized for certain practical applications. Expressions for the intensity and efficiency of the electron bremsstrahlung in dielectrics with an external electric field were derived in Ref. 79. It was shown that the maximum efficiency of the emission by runaway electrons is twice the value in the absence of a field. One is led to ask whether the gas or the anode is the primary source of radiation. Table V shows estimates of the intensity of the emission from the gas and from the anode (Al) at $U = 200$ kV and $P = 760$ Torr. We see that the source of the bremsstrahlung of the anomalous-energy electrons ($\varepsilon_m \approx 300$ keV) is the anode, as was assumed above. Secondary runaway electrons of relatively low energy emit primarily in the gas. Although the intensity of this radiation can be far higher than that of the bremsstrahlung of the anomalous-energy electrons, this radiation is completely absorbed in the anode because of the small value of $\bar{\varepsilon}_\gamma$, and it cannot be detected by the instruments.

6. PARTICIPATION OF THE RUNAWAY ELECTRONS IN THE DYNAMICS OF ELECTRIC DISCHARGES IN DENSE GASES

6.1. Volume discharges. High-energy conductivity. Contraction

High-voltage nanosecond volume discharges have been studied in several places[23,33,38,59,76,80,81] at pressures of the order of atmospheric and at high overvoltages Δ. A volume stage of the discharge, preceding the formation of a contracted channel, has been observed in several places.[3-5,45] A factor which hinders the achievement of a volume discharge is the formation of a cathode spot.[81] At $\Delta \gg 1$, however, a spot does not necessarily result in a contraction: At a current density $j(d) \approx 1$ kA/cm^2 at the anode, the volume nature of the discharge is disrupted only by small plasma formations near the cathode with an average current density $j_p \approx 100$ kA/cm^2 (Subsection 3.1). Volume discharges are accompanied by particularly intense acceleration processes and are apparently achieved as a result of these processes. On the basis of the experimental results presented in §2 and §3, the evolution of nanosecond volume discharges at large values of Δ can be described as follows.[38] As the pulsed voltage $U(t)$ across the discharge gap rises, a streamer forms near the cathode. It propagates toward the anode as a result of the runaway of some of the electrons near its front, with a subsequent slowing far from this front. As $U(t)$ rises, the electric field in the gap increases to the extent that the runaway electrons are accelerated to the anode, and no further formation of compact plasma regions is possible, since the gap is greatly preionized. In regions in which avalanches successfully develop, the avalanches overlap without converting into streamers. This effect is related to the diffuse appearance of the discharges. The number of anomalous-energy electrons detected is sufficient to provide the necessary preionization. According to (3), a runaway is possible only for small values of ψ as long as the relation $E_0 < E_{cr}$ holds. The "corona" of the plasma near the cathode is explained on the basis that as ψ increases in value there is an increase in the number of electrons which are not entrained in the runaway in the field $\mathbf{E}_0$ and which are capable of effectively ionizing and exciting the gas. Only as the value $\psi = \pi/2$ is approached does the number of these electrons begin to decrease.[33] The volume emission results from $C\,^3\Pi_u \to B\,^3\Pi_g$ transitions of the N_2 molecule. For runaway electrons with $\varepsilon \gg 1$ keV, the mean free path with respect to excitation of the $C\,^3\Pi_u$ state is $\lambda_{ex} > 50$ cm $\gg d$. The distribution of the emission is thus determined by the spatial distribution of the secondary electrons, whose average energy $\langle \varepsilon_{BT} \rangle \approx \varepsilon_1 [\ln(\varepsilon/\varepsilon_1) - 1]$ ≈ 100 eV depends only weakly on the point at which the electrons are generated, and we have $\lambda_{ex}^{BT}(C\,^3\Pi_u N_2) \approx 100$ mm. This figure corresponds to the length of the dark region which separates the plasma from the volume glow. The origin of the dark region is thus similar in nature to that for the Crookes dark space. The dark band observed near the cathode in Ref. 45 is apparently of the same origin. In the dark region, the field is so strong that the electrons undergo very few collisions with molecules, and the current is determined entirely by the motion of the runaway electrons. In this sense, a "limiting-voltage effect"[82] occurs locally, but in a dense gas. In high-voltage nanosecond discharges at $\Delta \gg 1$, in the region $P < 100$ Torr, the high-energy component of the conductivity is the greater part of the conductivity, since much of the accumulated charge Q_0 is carried by the runaway electrons. At pressures of the order of atmospheric, only the anomalous-energy electrons, with a charge $eN_e \lesssim 10^{-4}$ of Q_0, are detected. Since the anomalous-energy electrons are generated at the front of the first streamer, in a process matched with the current rise, and since the pulse length of these electrons is $\Delta t_e \lesssim \tau_I$, we can evaluate the conduction mechanism which involves a preionization of the gap by these electrons in a natural way. Taking into account the change in the energy of the secondary electrons, $\langle \varepsilon_{BT} \rangle / \varepsilon_{in}$, we can write the avalanche current at a point $x \in [0,d]$ in a gap with a gas particle density n_g as follows:

$$I_a(x) = eN_e \sigma_i(\varepsilon) n_g v_- \frac{\langle \varepsilon_{BT} \rangle}{\varepsilon_{in}} e^{\alpha v_- \tau_I}. \qquad (4)$$

Table VI shows distributions along the x axis in the gap of the basic quantities characterizing the development of avalanches.[38] If we assume $\sigma_i \approx 10^{-18}$ cm^2, $\langle \varepsilon_{BT} \rangle \approx 150$ eV, and $\varepsilon_{in} \approx 31$ eV, we find $I_a(d) \approx 500$ A for $r_c = 6$ mm or $I_a(d) \approx 0.5$ A for $r_c \approx 200$ μm. Far from the anode, $I_a(x)$ increases the more rapidly, the smaller is the curvature of the cathode.

One might attempt to explain the pronounced discrepancy with the measured value $I_m \approx 1$–2 kA at $r_c \approx 200\,\mu$m on the basis of the mechanism outlined above and by taking the space-charge field into account. However, the results of research on volume discharges show that acceleration processes may determine the conductivity of the gap at $P \approx 760$ Torr, as they do at low pressures. In the first place, the lower limit found for the ionization propagation velocity corresponds to an electron energy $\varepsilon \approx 1$ keV. Second, when a high power density is delivered to the gap, the only way to explain the anomalously slight heating of the main gas volume and the relatively low degree of ionization of the plasma near the cathode is in terms of a relatively weak interaction of the runaway electrons with the medium. Furthermore, it can be seen from Table VI that there is a fairly wide region with $E_0(x)/P \gtrsim (E/P)$. According to calculations based on (3), electrons produced near the cathode are accelerated in the field $E_0(x)$ to the anode. In other words, a substantial fraction of Q_0—the greater fraction in a configuration with $r_c \approx 200$ μm—is carried by runaway and secondary electrons. As the dense plasma near the cathode develops, conditions become more favorable for runaway in gaps with a relatively uniform electrode configuration ($l_p \ll r_c$), while conditions become worse in the case $r_c \ll l_p$, since the plasma screens the sharp cathode. The changes in the conditions for the development of avalanches are in the opposite direction. In each cross section of the gap outside the plasma near the cathode, the current of a volume discharge is a sum of three components: $I(x) = I_{ya}(x) + I_{Br}(x) + I_a(x)$, where I_a has a maximum whose position x_a in an isolated pulse moves off toward the anode with increasing $U(t)$. In a cross section near the plasma beside the cathode, the current is the sum of I_{RE} in the dark space and the current in the corona plasma. All three components exist at the anode, but in highly nonuniform configurations we would have $I_a(d) = 0$.

The conductivity of nanosecond volume discharges is thus determined both by runaway and secondary electrons, on the one hand, and the preionization of the gap by the anomalous-energy electrons, on the other. There is a subsequent avalanche breeding in either case. The relative importance of one mechanism or the other depends on the particu-

TABLE VI.

x, mm	$r_c = 6$ mm, $d = 2$ cm, $U_m = 240$ kV				$r_c \approx 200\,\mu$m, $d = 2$ cm, $U_m = 200$ kV			
	E_0/P, V/(cm·Torr)	$e^{\alpha v_- \tau_I}$ 10^4	z_{cr}, μm	t_{cr}, ns	E_0/P, V/(cm×Torr)	$e^{\alpha v_- \tau_I}$	z_{cr}, 0.1 mm	t_{cr}, ns
0	436		4,3	0.04	4345			
0.5	376		50	0.06	750			
1	329		56	0,07	408			
3	225		80	0,13	152	10^{14}	1.6	0.3
4	199		94	0,16	119	$5.3\cdot10^4$	3.0	0.8
6	162		130	0.25	84	28	8.4	3.0
8	134	10^4	220	0.51	67	3,0	18	10
10	125	765	260	0.63	58	1.8	34	18
20	101	0,1	470	1,4	43	1.1	192	133

TABLE VII.

x, mm	E_0/P, V/(cm·Torr)	αv_-, ns^{-1}	z_{cr}, mm	t_{cr}, ns
0	225	121	0,1	0,2
1	135	36	0,2	0,6
4	66	2,2	1,8	9,4
10	37	0,05	48	392
20	29	0,006	350	3600

lar experimental conditions, primarily the field configuration.

Kunhardt and Byszewski[34] suggest that a contracted channel forms at small values of Δ, as a consequence of ionization of the gas by electrons which are runaways in the intensified field at the front of the avalanche and which relax to $v_-(E_0)$ far from this front. Only at $\Delta > 1$ do the runaway electrons reach the anode, with the result that a volume discharge occurs. Actually, the spatial structure of discharges is determined not only by the overvoltage but also by the values of P, d, U_m, C_{gen}, and L_{gen}; the type of gas; and the field configuration. The participation of the runaway electrons in forming the structure of a discharge and its dependence on Δ is thus far more complicated. In Subsection 4.4, for example, we described a discharge with $\Delta \approx 0.6$ which did indeed contract, but nevertheless runaway electrons with $\varepsilon \approx eU_m$ were detected beyond the anode. Table VII characterizes the growth of avalanches in this discharge:[39] $d = 2$ cm, $r_c = 3$ mm, $U_m \approx 80$ kV. We see that the relation $E_0(x)/P < (E/P)_{cr}$ holds; i.e., a field intensification is a fundamental necessity for the acceleration of electrons. Although the runaway electrons preionize the gap, avalanches whose overlap might hinder contraction do not have time to develop far from the cathode ($x > 1$ cm). On the other hand, as Δ increases, the discharges may, after passing through a volume stage, contract again at very large values of Δ. For example, nanosecond high-voltage volume discharges in air at $P = 760$ Torr become contracted as d decreases. A reduction of d by a factor of 7 reduces U_m by a factor of less than 2 (Table III); i.e., the overvoltage increases, as does E. At small values of r_c, this occurs far from the cathode for the most part. A contracted channel is apparently preceded by a volume stage. The many experiments which have been carried out on nanosecond high-voltage discharges in air at atmospheric pressure lead to the following conclusions: A contracted channel forms if there is a sufficiently strong field, and the probability for the formation of a contracted channel increases with the uniformity of the field. At sufficiently small values of d, the measured value of I_m can be accounted for entirely by the preionization of the gas by anomalous-energy electrons, followed by avalanche breeding. The contracted channel grows from the cathode in a plasma with a fairly high degree of ionization. Because of the screening of the field by the plasma, the field ahead of the channel front, E_f, can reach the values required for intense ionization of the gas over a time $\lesssim 1$ ns.

Beginning at certain sufficiently large values of E_0/P, the formation of a contracted channel may be due to a runaway of essentially all the electrons near the head of the channel, including the electrons near the maximum of the ionization cross section σ_i^m. The runaway condition then doubles as the condition for breakdown according to the conventional definition of the word. When a displaced Maxwellian velocity distribution is used for the electrons, and when the Born approximation is used for the friction force, one finds the following condition for electron runaway:[39]

$$\frac{E}{P} > \left(\frac{E}{P}\right)^* = \frac{Ze\Lambda_{in}G^m}{4\pi\varepsilon_0 d_{g1}^2}, \tag{5}$$

where $d_{g1}^2 = \varepsilon_0 T_e/n_{g1}e^2$, n_{g1} is the density of gas particles at $P = 1$ Torr, Λ_{in} is the average value of the logarithm in the Bethe formula for the inelastic energy loss, G^m is the maximum value of the Chandrasekhar function, and $\varepsilon_0 = 10^7/4\pi c^2$ F/m. If we assume $T_e \approx 10$ eV, i.e., if we assume that this temperature is equal to the average energy of the electrons in the avalanches at large values of E_0/P (Ref. 83), and if we set $\Lambda_{in} = 1$, then we find $(E/P)^* \approx 2$ kV/(cm·Torr) in air. For energies near σ_i^m we find $E/P \approx 200$ V/(cm·Torr). Both of these estimates are close to the value of E_0/P in the cathode region of a high-voltage nanosecond discharge in a dense gas at a high overvoltage (Table VI). Condition (5) holds particularly well at the front of a channel growing out of the plasma beside the cathode in the volume forms of these discharges as d is reduced.

6.2. Electron runaway and the *U*(*Pd*) dependence

A self-sustaining gas breakdown on the left-hand branch of the Paschen curve $U_s(Pd)$, in the region $Pd \ll (Pd)$, is known to develop in a regime of electron runaway. In this region we have $E_s = U_s/d \gg E$, and the initial stage is typically a volume stage. It was established in Refs. 60 and 62 on the basis of the runaway condition and the data in Table I that the condition $eU_s^{min} > \varepsilon_{m1}$ holds for static breakdown. That condition means that some of the electrons can in principle overcome the loss maximum $L_1^m P$. For all gases except He the condition $(eE_s/P)_{min} > L_1^m$, holds; i.e., the runaway condition holds on the entire left-hand branch of the $U_s(Pd)$ dependence, even if E_p is ignored. The values of $(eE_s/P)_{min}$ are close to L_1^m, except in very electronegative gases. Figure 18 shows $U_s(Pd)$ in air and He, along with $E_s(Pd)/P$ in air. The values of $E_s/P = L_1^m/e$ and $(E_s/P)_{min}$ are shown here. The function $E_s(Pd)/P$ decreases monotonically with increasing Pd, and a necessary condition for electron runaway at $Pd > (Pd)_{min}$ is a local intensification of the field by space charge. This condition underlies the classical streamer model for $Pd \gtrsim 200$ Torr·cm. If one assumes $(E/P)_{min} = (U/Pd)_{min} \approx L_1^m$ = const for a given gas, then an increase in Δ should be accompanied by an increase in $(Pd)_{min}$; i.e., an increase in Δ (a decrease in the rise time τ_{gen} of the voltage pulse) should be accompanied by a rightward shift of the minimum of $U(Pd)$. Figure 18 shows measurements of $U(Pd)$ for $d = 1$ cm in an approximately plane-parallel geometry.[62] Curve 4

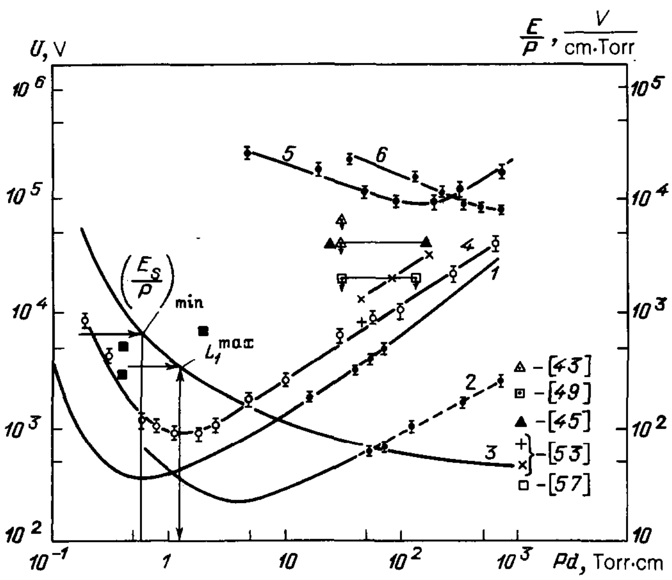

FIG. 18. The functional dependence $U(Pd)$. Static case: *1*–Air; *2*–helium. E_s/P: *3*–Air; *4*–microsecond pulse in air. Nanosecond pulse: *5*–Air; *6*–helium.[60,62] ■–According to Ref. 57.

was found during the breakdown of air by microsecond pulses with exposure to UV light ($\Delta = 0.3$ at $P = 760$ Torr). Curves 5 and 6 correspond to discharges at large values of Δ ($\tau_{\text{gen}} < 0.6$ ns, $\Delta t_u = 5 - 8$ ns, $U^{\text{m}}_{\text{gen}} \approx 250$ kV). The discharges begin at the front of the voltage pulse and develop in an electron runaway regime over the entire range of P.

To the left of the minimum, the discharges are volume discharges; to the right, a contracted channel gradually forms with increasing Pd. After a certain value of Pd is exceeded, the discharges become volume discharges again. Curves 4–6 have the shape characteristic of Paschen curves 1 and 2, with a characteristic minimum. The position of this minimum can shift to larger values of Pd. Note the approximate equality of the values of $U_{\min}/(Pd)_{\min}$ for all curves 1, 4, and 5. This approximate agreement means that a necessary condition for the acceleration of electrons to the right of the minima on curves 4 and 5 is a local intensification of the field by space charge, as in the static case. Shown here and in Table VIII are data from studies which detected x radiation in plane-parallel gaps. The arrow means that U_{m} was not measured during the breakdown; i.e., the condition $U_{\text{m}} > U^{\text{m}}_{\text{gen}}$, shown in Fig. 18, may hold. Interestingly, the single point from Ref. 53 essentially coincides with curve 4 for a microsecond pulse, in the region $(Pd)_{\min} < Pd < 200$ Torr·cm. The overvoltage at this point is only $\Delta \simeq 1$. The observation of soft x radiation during breakdown on the right-hand branch of $U_s(Pd)$ would make it possible to combine conclusively all regimes of spark breakdown of dense gases on the basis of a common mechanism. If such experiments are to succeed, they will require methods for detecting radiation which are more sensitive than those which have been used in the published studies.

7. MECHANISM FOR THE GENERATION OF ANOMALOUS-ENERGY ELECTRONS

Fast unthermalized particles are typical of hot plasmas. Their presence is usually correlated with the excitation of plasma instabilities. The time scales of the acceleration mechanisms which involve these instabilities, however, are greatly at odds with experimental data on high-voltage nanosecond discharges in dense gases at high overvoltages. Stochastic acceleration in the dense plasma near the cathode in a discharge, for example, requires $T_e \approx 200$ eV (Ref. 84). Experiments carried out to detect thermal x radiation from the plasma beside the cathode, corresponding to a temperature $T_e \sim 100$ eV, have yielded negative results.[23] Acceleration in the vortical electric fields generated during the development of the necks in the hypothetical micropinches near the cathode, which may form near emission spots, would require collapse velocities comparable to the velocity of light, but such velocities are unlikely in dense gases under the conditions prevailing in nanosecond discharges. Furthermore, the development of necks is suppressed by the breakdown of the gas between adjacent thickening regions.

In a dense gas with a strong electric field, the mechanism for the generation of anomalous-energy electrons which appears to be the most natural is that which is associated with an extremely high rate of ionization: polarization self-acceleration of charged particles.[28-30] That mechanism was outlined in the Introduction to this review, as the result

TABLE VIII.

Reference	P, Torr	d, cm	τ_{gen}, ns	$U^{\text{m}}_{\text{gen}}$, kV	Δt_{gen}, ns
[43]	760, air	0,04	2	40—58	23
[45[	30, air	1—6	<2	40	40, 100
[49]	76—760, N_2	0,4	3	20	150
[53]	500, N_2	0.5		20—30	45
[57]	10, air	0.1	50	3—12	

of an extrapolation of the first of the three ideas underlying the streamer model to the region of overvoltages of a large factor. Since the anomalous-energy electrons are detected at the current front, $\Delta t_e \lesssim \tau_I$, and their number is $N_e \sim N_e^{(cr)}$, their generation can be explained on the basis of the mechanism of polarization self-acceleration at the front of a primary streamer of length $l_{str} \ll d$, which develops near the cathode during the rapid increase in the conduction current.[35,36] If the streamer is approximated as an ideally conducting semiellipsoid of revolution, which is stretching out from the cathode surface ($x = 0$) in the direction opposite to that of $\mathbf{E}_0$, then the field in Eq. (3) with $\psi = 0$ can be described by

$$E_f(\xi, 0) = E_0 + E_0 \left(f\left(\frac{l_c}{r_c}\right) - 1 \right) \left(1 + \frac{\xi}{l_c} \right)^{-3}. \qquad (6)$$

Here l_{str} and $2r_{str}$ are the length and thickness, respectively, of the streamer; ξ is reckoned from the streamer surface, which is to be understood as the surface with $E_f(\xi,\psi) = E_f^{max}$; and $f(l_{str}/r_{str})$ is the field intensification factor. We assume that the electron runaway condition $E_f^{max} \geqslant E_{cr}$ becomes satisfied at the streamer front at a time t_0 with respect to the application of the voltage pulse. Since l_{str} increases over time in an accelerated manner according to the first of the three streamer-model ideas, the runaway electrons at the point $x = l + \xi$ "observe" a field stronger than the field which existed at this point at the time at which these electrons started from the streamer surface. In the limit in which the polarization of the streamer plasma and the displacement of the field occur so rapidly that the velocity of the runaway electrons and $\dot{l}_{str}$ become equal, there can be a synchronized motion of the maximum of the intensified electrostatic field $E_f^{max} = E_f(\xi = 0, \psi = 0)$ at the streamer front, (a field soliton) and of the electrons accelerated in the field. Since the runaway electrons preionize the gas ahead of the streamer front, a soliton with a growing E_f^{max} is in a sense transported by the runaway electrons themselves: There is a self-acceleration. We denote the position of the front of the runaway-electron flux with respect to the cathode by:

$$x_e(t) = \int_{t_0}^{t} v_e(t')\, dt'.$$

The position of E_f^{max} is then given by, according to Fig. 1 (Refs. 35 and 36),

$$l_{str}(t) \approx x_f(t) = x_e(t - \tau) + \int_{t-\tau}^{t} v_-(t')\, dt' \approx \int_{t_0}^{t-\tau} v_e(t')\, dt' + \int_{t-\tau}^{t} v_-(t')\, dt', \qquad (7)$$

where $\tau(t)$ is the time scale of the screening of the field E_f due to the drift of the electrons at the front, moving at a velocity $v_-(E_f)$.

In the quasineutral region $x \lesssim x_f(t)$, where the field is weak, a conduction current of density $en_e \mathbf{v}_-$ flows. In the interval $[x_f(t), x_e(t)]$, there is an intense ionization, and there is a drift of electrons at the velocity $v_-(t)$, which causes a polarization of the plasma and a displacement of the field toward the anode at a velocity $v_f(t) \approx \dot{x}_f(t) = \dot{l}_{str}$. Here the current density is $en_e \mathbf{v}_-(E_f) - \varepsilon_0 \partial \mathbf{E}_f/\partial t$. In the region $x > x_e(t)$, only a displacement current flows, with a density $\varepsilon_0 \partial \mathbf{E}_f/\partial t$.

Introducing the length of the ionization wave,

$$\lambda(t) = x_e(t) - x_f(t) = \int_{t-\tau}^{t} v_e(t')\, dt' - \int_{t-\tau}^{t} v_-(t')\, dt' \qquad (8)$$

and differentiating it under the condition that the motion of the runaway-electron front is synchronized exactly with the streamer surface $\lambda = $ const, we can write

$$\frac{\Delta v_e}{v_e(t-\tau)} = \frac{v_e(t)}{v_e(t-\tau)} - 1 \approx -\dot{\tau}, \qquad (9)$$

In other words, a polarization self-acceleration ($\Delta v_e > 0$) is possible if $\dot{\tau} < 0$. In the opposite case, the runaway electrons detach from the soliton ($v_e > \dot{l}_{str}$), and the synchronization is disrupted. The value of λ must be small enough to satisfy the condition $E_f(x_e) \approx E_f^{max}$. If the synchronization is maintained, the energy of the runaway electrons depends strongly on the streamer length[30] $l_{str} \approx x_f(t)$. If we assume[12] $f(l_{str}/r_{str}) \approx (l_{str}/r_{str})^2$ where[12] $r_{str} \approx$ const, if we assume $\xi = \lambda \ll l_{str}$, and if we ignore the energy loss, then we find from (3) and (6)

$$\Delta\varepsilon \approx e \int_{l_{str}(t_0)}^{l_{str}(t)} dl'_{str} E_f(l'_{str}) \approx eE_0 \left(\frac{l_{str}}{r_{str}}\right)^2 \frac{l_{str}}{3}. \qquad (10)$$

The flux of runaway electrons, N_e/S_e, causes a preionization $n_e(0) \approx N_e \sigma_i n_{g1} P/S_{str}$ over a distance λ ahead of the frontal surface of the streamer, with an area $S_{str} \sim \pi r_{str}^2$. Assuming $v_- = \mu_-(E_e/P) E_f/P$, where the electron mobility is[83] $\mu_- = \text{const} \cdot (E_f/P)^{-\nu}$, and $n_e(t) = n_e(0)\exp(\alpha v_- t)$, we find the expression $\alpha v_- \tau \approx \ln(\tau_{\alpha=0}/\tau)$ from the condition for the screening of the field E_f by the plasmawhich is forming: $en_e v_- \tau/\varepsilon_0 \approx E_f$. The time scale of this screening in the case $\alpha = 0$ is[36]

$$\tau_{\alpha=0} = \frac{E_f}{E_e} \frac{\alpha\lambda_i}{2\alpha v_-}.$$

Here $E_e = eN_e/2\varepsilon_0 S_{str}$ is an estimate of the self-field of the runaway electrons, and $\lambda_i = 1/n_{g1}\sigma_i P$. We then find

$$\dot{\tau} = \frac{\tau}{1 + \alpha v_- \tau} \left[\left(\frac{\dot{\tau}}{\tau} \right)_{\alpha=0} - \tau \frac{d}{dt} \alpha v_- \right]. \qquad (11)$$

For $eE/P \gtrsim L_I^m$ in air we would have $\alpha v_- \sim E/P$ and $\nu \approx 0.5$ (Refs 12 and 83). Again assuming $E_f \approx E_0 (l_{str}/r_{str})^2$, where $r_{str} = $ const and $\sigma_i \approx \text{const}/\varepsilon$, we find

$$\dot{\tau} \approx \frac{2}{1 + \alpha v_- \tau} \frac{v_{str} \tau}{l_{str}} (2 - \alpha v_- \tau). \qquad (12)$$

Since we have $\alpha v_- \tau = \ln(\tau_{\alpha=0}/\tau) \approx \ln(E_f \alpha\lambda_i/2E_e)$, accurate up to the operation of taking logarithms twice, we have $\dot{\tau} < 0$, according to (12), under the condition

$$\left(\frac{E_f}{E_e}\right) \alpha\lambda_i > 2e^2 \approx 15. \qquad (13)$$

In very strong fields E_f, in which all the electrons at the streamer front run away, condition (13) may be violated, because $E_f/E_e \to 1$ and $\alpha\lambda_i \to 1$. If there is no avalanche breeding ($\alpha = 0$), the condition $\dot{\tau} > 0$ holds at all times.[36]

The runaway electrons thus initiate undamped avalanches in a volume $\sim\pi r_{str}^2\lambda$. Under condition (13), these avalanches synchronize the motion of the runaway electrons and the electrostatic-field soliton, which are in a sense coupled chains of avalanches.[36] A necessary condition for the formation of these chains is $n_e(0)\pi r_a^2 z_{cr} \geqslant 1$. We thus find a lower limit on the number of runaway electrons:

$$N_e \geqslant N_e^{min} \approx \frac{l_{str}^2}{6z_1 z_{cr}} \frac{eU_m}{T_e} \frac{\lambda_1}{d}, \qquad (14)$$

where z_1 is the distance traveled by an avalanche before the beginning of ambipolar diffusion. Here, in contrast with Ref. 36, we have made use of the circumstance that in strong fields the maximum avalanche radius r_a is[85] $rD_-(z_1)$ and is not limited to a value[12] $1/(2\alpha)$.

A limitation stronger than (14) on the number of runaway electrons stems from the self-field of the space charge, $E_e \ll E_f$, or[36]

$$N_e \ll N_e^{max} \approx \frac{2\varepsilon_0 E_f S_{str}}{e} \approx \frac{2\pi\varepsilon_0 U_m l_{str}^2}{ed}. \qquad (15)$$

Assuming $l_{str} \approx l_p \approx 1$ mm (Subsection 3.1), $U_m \approx 200$ keV, and $d = 2$ cm (Table III), we find from (10) that the anomalous-energy electrons acquire an excess energy $\Delta\varepsilon = \varepsilon_m - eU_m \approx 100$ keV over a distance $l_p \ll d$ if the condition $l_{str}/r_{str} \approx (3d\,2l_{str})^{1/2} \approx 5$ holds. This condition is completely realistic. The dark space (Subsection 3.1) and the termination of self-acceleration result from an intensification of the field at the streamer front which occurs when the electrons at the front reach energies in the region of the incident energies, $\sigma_i(\varepsilon)$, over one mean free path and are scattered out of the effective range of the soliton without initiating avalanches and without causing any significant excitation of the gas. When we then assume $\sigma_i(100\ \text{keV}) \sim 10^{-18}$ cm^2, $\alpha/P \sim 10$ cm$^{-1}\cdot$Torr^{-1}, $\alpha z_1 \approx \alpha z_{cr} \approx 10$, and $T_e \approx 10$ eV, we find the estimates $[N_e^{min}, N_e^{max}] \approx [4\cdot 10^5, 4\cdot 10^9]$ from (14) and (15). In other words, the number of anomalous-energy electrons detected, $N_e \approx 10^8 - 10^9$ (§4), lies in the interval defined by the limitation associated with the self-field of the space charge and the requirement that there be sufficient preionization ahead of the streamer front. The estimate of N_e^{min} is much too low, since in fields $E \gg E_{cr}$ the ionization is not described by the Townsend coefficient α. The duration of the acceleration is[35]

$$\Delta t \approx \int_{l_0}^{l_p} v^{-1}\,dl' \approx 20\ \text{ps} \ll \tau_I.$$

These estimates provide evidence that the concept of a polarization self-acceleration does not contradict experimental data on the dynamics of discharges in dense gases at high overvoltages with anomalous-energy electrons. The results of Refs. 23, 33, 50, 51, 54, 61, and 78 constitute the first observations and studies of the polarization self-acceleration of charge particles which was predicted by Askar'yan.[28-30] A nontrivial aspect of this effect is that it occurs only in dense gaseous media. At reduced pressures, at which the rate of dissipative processes falls off, the effect fades away. In this sense, polarization self-acceleration is analogous to the self-focusing of light and sound waves.[86] At first glance, polarization self-acceleration of electrons would appear to be an exotic mechanism, which would operate only in a dense gas at a high overvoltage. However, the acceleration motion of streamers under the condition $\Delta \ll 1$, under which the classical Raether model holds,[9-12] is essentially a polarization self-acceleration, but under conditions such that there is time for the attainment of a local equilibrium between the average electron energy $\langle\varepsilon\rangle$ and $E_f \approx E_0(l/r)^2$, which increases more rapidly than $\langle\varepsilon\rangle$. In N_2 at $20 \lesssim E/P \lesssim 100$ V/(cm·Torr), for example, we have $\langle\varepsilon\rangle \sim E_f^{2/3} \sim l^{4/3} < l^2$. A fundamental distinction between the Raether model and Askar'yan's mechanism is that in the former case the electrons undergo a drift motion ($E_f \ll E_{cr}$), while in the latter case they undergo a continuous acceleration ($E_f > E_{cr}$) and can acquire an energy $\varepsilon > eU_m$.

8. PHYSICAL PROCESSES NEAR THE CATHODE

The rise time of the current pulse is the sum of three components:[32] $\tau_I = t_s + t_{cr} + t_p$, where t_s is the statistical delay time, and t_p is the time required for the production of the plasma near the cathode and of the cathode spot, reckoned from the time at which the avalanche reaches critical dimensions, before the beginning of explosive electron emission. Corresponding to each of these components is a characteristic size of a spatial region with a field $E \sim 10$–100 MV/cm. Since $\tau_I < 0.5$ ns, we see that t_s, t_{cr}, and t_p fall in the picosecond range. In this range, gas breakdown is initiated by field emission from a few elongated microscopic protuberances or whiskers.[3,4,31] These whiskers have a reduced work function φ under the condition that a field $E_\mu \approx 20$–100 MV/cm is reached near their tips. Babich *et al.*[32] have carried out a model-based calculation of one-electron intiation of a high-voltage nanosecond gas discharge at a high overvoltage, without making use of such customary estimated characteristics[3,4] as the field intensification $\mu = E_\mu/E_0$ or the effective emitting surface area of a whisker, S_μ. They showed that a region near the tip of the whisker, consisting of a small number of atoms, does the emitting. For the emission of a single electron over a time $t_s \lesssim 1$ ns, there would have to be whiskers having a height-to-thickness ratio $a/2b \approx 10$–20 if $\varphi = 2.6$–4.5 eV. Because of the uncertainty in the microscopic surface relief of the cathode, the customary use of a semi-ellipsoid of revolution to model a whisker makes the calculation rather arbitrary.[32] As a result of the development of a net space charge of positive ions near a whisker which has initiated an electron avalanche, over a time $\sim t_{cr}$, the field intensifies, and neighboring microscopic protuberances also start emitting.[32] The intensity of the field emission near the site of the first ionization events is higher than the average intensity over the cathode, and it increases in a self-consistent fashion with E_{p+}. As a result, the emission current localizes at a small spot, and the plasma near the cathode is produced in a manner which is coordinated with the development of this small spot. The process is of the nature of an emission-ionization instability. Over a fraction of a nanosecond, a "quasianode" consisting of a cloud of positive ions thus forms near the cathode. There is a transition to thermal-field emission, and after a certain delay t_{pre} the emitting microscopic proturberances of a cathode sapo explode. In other words, an explosive electron emission occurs in the gas.[23,32,58,59,76,87] As was shown in Ref. 88, the electron emission and the development of the conductivity of the region near the cathode are strongly influenced by such processes as the surface migration of atoms and molecules toward the tips of microscopic protuberances, the reconstructing of surface layers of adsorbed gases and vapors, and the desorption of these gases and vapors. There is the possibility of a many-electron initiation of nanosecond gas discharges as the result of a breakdown of dielectric films.[87,88]

Experimental studies have been carried out on the effect of gaseous and explosion plasmas on emission processes for the conditions prevailing in high-voltage nanosecond gas discharges in dense gases at high overvoltages.[23,58,59] Cathodes with an extended working surface ($r_c = 3$–6 mm) have been used; this surface has been polished, or, on the contrary, notches have been made in it. In air at $P \approx 760$ Torr, plasmas regions near the cathode (Subsection 3.1) form, no matter what the surface state of the cathode. If $P \approx 10^{-3}$ Torr, a plasma is produced only in the case of notched cathodes. In gaps with polished cathodes at $P \approx 10^{-3}$ Torr, discharge phenomena (currents, plasmas, and x-ray emission) and manifested as d is reduced to the value at which E_0 is larger by a factor of 3–5 than at $P \approx 760$ Torr. As was mentioned back in Subsection 3.1, the breakdown delay time t_d, which is reckoned from the beginning of the flow of the bias current I_b, decreases with increasing P (Fig. 8). These results are convincing evidence that the field is intensified by the positive space charge of the air plasma and that ions of this plasma participate in the electron emission. At sufficiently high pressures, explosive processes near a cathode spot are initiated by a gaseous plasma, as follows from time-resolved spectral measurements of the emission from the plasma near the cathode (Subsection 3.2). We should add that in high vacuum ($P \lesssim 10^{-7}$ Torr) a plasma is not produced near the cathode in a gap with a cathode made of the VNM (W-Ni-Cu) alloy. Only four atomic lines of WI are observed in the emission spectrum of the cathode region. These lines are the same as are observed in air at $P = 760$ Torr. In order to detect the spectrum of the discharges in vacuum, it has been necessary to increase the number of pulses by a factor of 100 (Ref. 88). Figure 19 shows photomicrographs of the working surface of a cathode.[59] We see microscopic craters ~ 1–$10\ \mu$m in diameter, arranged in groups around marks left by the mechanical treatment (Fig. 19a). We also see some isolated microscopic craters, surrounded by a melted surface (Fig. 19b). On a nickel cathode, the central lune is surrounded by a zone whose temperature rises sharply during the discharge (Fig. 19c). The nature of the erosion depends on both the pressure and the thermodynamic characteristics of the metals. At reduced pressures, the erosion is less pronounced (Fig. 19d). Either a single microscopic crater or many microscopic craters, smaller in size, can form in a single pulse. When there are numerous craters, they are arranged at random over the surface of the cathode or concentrated near marks left by the processing. The heating of the cathode near the microscopic craters stems from the heat flux from the center of a microscopic explosion, ion bombardment, and emission from the plasma near the cathode. No erosion has been observed at the anode. The explosive change in the microscopic relief of the cathode surface was caused primarily by a pulsed heating of the microscopic protuberances by the thermal-field emission current of critical density.[4,58,59] Since the total area of the emission spots is $S_{em} \approx 10^{-6}$ cm^2 (Fig. 19b), and since we have $I_m \approx 1$–2 kA, the emission current density is $j_m \approx I_m / S_{em} \approx 1$ TA/cm^2. This figure agrees with the density of the preexplosion current for Ni and Zn, estimated from $j_{cr}^2 t_e \approx 2 \cdot 10^9$ A^{2}s/cm^4 with $t_e \sim t_p \approx 0.1$ ns. In addition to the Joule heating of the microscopic emitter, one should take into account the shock heating by ions of the discharge plasma; these ions acquire a significant energy in the intensified field near a microscopic protuberance which focuses ions.[58,59] This factor is quite important in promoting an explosive electron emission in the gas discharge.

The role played by the explosion plasma in the development of high-voltage nanosecond discharges in dense gases at high overvoltages is thus more modest than that in vacuum discharges. Further evidence for this conclusion comes from the fact that the conduction current reaches its maxi-

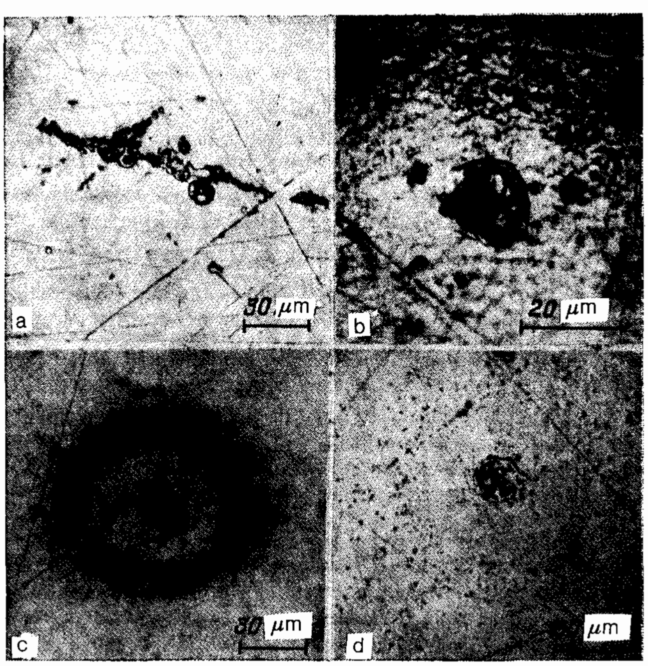

FIG. 19. Photomicrographs of regions on the surfaces of cathodes. a–Zn, 50 pulses, $P = 760$ Torr; b = Zn, 1 pulse, $P = 760$ Torr; c–Ni, 50 pulses, P = 760 Torr; d–Zn, 50 pulses, $P = 40$ Torr ($U_{gen}^{m} = 250$ kV, air, $d = 15$ mm, $r_c = 6$ mm; Ref. 59).

mum before the metal lines appear in the spectrum of the plasma near the cathode.[23] In other words, the explosion processes are playing a secondary role, and the plasma of the gas is the factor of primary importance in stimulating electron emission from the cathode.[58,59]

9. MECHANISM FOR THE DEVELOPMENT OF DISCHARGES IN DENSE GASES AT HIGH OVERVOLTAGES

According to the research results presented above, the dynamics of high-voltage nanosecond discharges in dense gases at high overvoltages can be outlined as follows. Field emission of a few electrons initiates an electron avalanche. This avalanche develops at the front of the voltage pulse. Over a time of the order of hundreds of picoseconds, and over a distance $z_{cr} \sim 100$ μm, it converts into a streamer, directed toward the anode. Before the voltage pulse reaches its maximum value, the electric field at the front of the streamer reaches a critical value E_{cr}. At this critical value, runaway electrons appear, and Askar'yan's mechanism of polarization self-acceleration comes into play. It leads to the generation of a subnanosecond pulse of anomalous-energy electrons. These electrons preionize the electrode gap, giving rise to volume discharges in gaps with a relatively uniform field. In highly nonuniform fields, volume discharges form solely as a result of ionization of the gas by the flux of runaway electrons. Since the gap width satisfies $d \gg z_{cr}$, the propagation of ionization toward the cathode is supported not so much by preionization of the gas by emission from excited atoms[9,17] and by bremsstrahlung of avalanche electrons[89] (and then by electrons of the streamer and the runaway electrons) as by the photoelectric effect at the cathode.[90,91] The local field intensification at the cathode by the positive space charge of the ions, which occurs in a manner coordinated with the development of ionization and emission processes, gives rise to a plasma region at the site of the first avalanche in a time $t_p \lesssim 1$ ns. The formation of this plasma region is accompanied by the development of a cathode spot and by explosion processes on the cathode, with a transition to an explosive electron emission. At sufficiently small values of d (at sufficiently high values of the external electric field E_0), the plasma transforms into a contracted channel, which grows, if there is a continuous preionization of the gas by the flux of runaway electrons. Because of the huge value of the local field, the head of the channel, at which the negative space charge is concentrated, is accelerated as a whole. Although it has been found possible to deliver a power density ~ 100 MW/cm^3 to a gas-discharge gap, the plasma remains a low-temperature, weakly ionized plasma throughout the evolution of the discharge, because of the weak interaction of the runaway electrons with the gas. The statistics of this interaction and the statistics of the initiation of electron avalanches explain the diversity of spatial forms of the discharges.

10. CONCLUSION

Mesyats *et al.*[3] concluded their earlier review with the following words: "This type of discharge, however, has not yet received much study." They meant discharges in dense gases at $E_0 \approx 100$ kV/cm. In 1972, only a few studies of this topic had been published.[18,43,44,48,49,75,90,92,93] The apparatus for generating high-voltage pulses with subnanosecond rise times which was developed in the 1960s made it possible to push research on gas discharges into the region of stronger fields. Since that time, systematic studies have been carried out, and these studies have radically changed our understanding of the physics of the breakdown of high-overvoltage gas-filled gaps at Pd values to the right of the minimum on the Paschen curve $U_s(Pd)$. It has been found that there are only a limited number of basic principles underlying the classical models of the electric breakdown of dense gases, which are actually constructed on the basis of a local diffusion-drift approximation of the equations for the moments of the electron distribution function.[9-12] At high overvoltages Δ, the concept of "locality" loses its meaning. The basic principles of a nonlocal mode of the breakdown of dense gases in gaps with high overvoltages were formulated not in 1980 (Ref. 34), as was asserted in Ref. 91, but much earlier.[27] Work in this direction was initiated some time ago by the paper published by Stankevich.[18] It turned out that at $\Delta \gg 1$ the electron runaway effect plays a fundamental role in the breakdown mechanism and in the entire dynamics of pulsed discharges in dense gases. The participation of runaway electron in the breakdown of dense gases can be seen in the shift of the minimum on the $U(Pd)$ curves with increasing Δ (in the decrease in the rise time of the voltage pulse, τ_{gen}) at large values of Pd. The dielectric strength of gases is thus characterized by a single-parameter family of $U(pd,\tau_{gen})$ curves, where τ_{gen} is a parameter. Yet another fundamental dependence $U_{min} = f((Pd)_{min}) \approx (E/P)_{cr}(Pd)_{min}$, arises here; it is clearly worthwhile to measure this dependence for various gases. Several arguments, including some which follow from direct experiments, constitute a quite convincing case that runaway electrons participate in the dynamics of pulsed discharges beginning at relatively low values of Δ, and the hypothesis of photoionizing emission in the mechanism for the breakdown of gas-filled gaps with an overvoltage becomes extraneous over a wide range of conditions. In order to identify the boundary on the region of applicability of the nonlocal model, it is necessary to study the electron runaway effect at small values of Δ and to study the photoionization of gases by photons with $\hbar\omega \sim \varepsilon_i$ at $\Delta \gg 1$. The simplest way to achieve E_{cr} in a dense gas near $U_s(Pd)$ is to use a highly nonuniform electrode configuration. Of particular interest for the physics and technology of high-voltage, high-pressure switches would be to advance the research on acceleration processes into the range of pressures above atmospheric. Acceleration processes are effective in systems for initiating and pumping high-power, high-pressure gas lasers.[6-8,64,94] Electron accelerators which operate on the basis of a high-voltage glow discharge at $P < 1$ Torr are used in several practical applications.[95-98] As was shown above, the boundary of the region of intense electron runaway, P_{run}, shifts to a higher pressure as Δ is increased. With the help of a system for forming high-voltage pulses with τ_{gen} shorter, and with a steepness $\dot{U}_{gen}$ greater, than in the given study, it would be possible to develop an efficient electron accelerator which operates in air at atmospheric pressure. The development of such systems is a scientific-technological problem which deserves attention now. The solution of this problem would make it possible to realize more fully the capabilities of the mechanism of polarization self-acceleration of charged particles in dense gaseous media. This mechanism is manifested even in the dynamics of classical streamers at $\Delta \ll 1$, as a drift motion of electrons at the streamer front. In the form of a purely accelerated motion of a stream of electrons, this mechanism is realized as the generation of anomalous-energy electrons in a dense gaseous medium, as was first observed in a study of the breakdown of air-filled gaps at atmospheric pressure with a high overvoltage.

We wish to thank V. I. Karelin, who took on the task of reading this manuscript and who has pointed out errors.

[1]M. Neuman, Phys. Rev. **52**, 652 (1937).

[2]R. C. Fletcher, Phys. Rev. **76**, 1501 (1949).

[3]G. A. Mesyats, Yu. I. Bychkov, and V. V. Kremnev, Usp. Fiz. Nauk, **107**, 201 (1972) [Sov. Phys. Usp. **15**, 282 (1972)].

[4]Yu. D. Korolev and G. A. Mesyats, *Field-Emission and Explosi n Processes in Gas Discharges* [in Russian], Nauka, Novosibirsk, 1982.

[5]B. M. Koval'chuk, V. V. Kremnev, and Yu. F. Potalitsyn, *High-Current Nanosecond Commutator Switches* [in Russian], Nauka, Novosibirsk, 1979.

[6]A. I. Pavlovskiĭ, V. S. Bosamykin, V. I. Karelin, and V. S. Nikol'skiĭ, Kvant, Elekctron. (Moscow) **3**, 601 (1976) [Sov. J. Quantum Electron. **6**, 321 (1976)].

[7]A. I. Pavlovskiĭ, V. F. Basmanov, V. S. Bosamykin, V. V. Gorokhov, V. I. Karelin, and P. B. Repin, Kvant. Elektron. (Moscow) **14**, 428 (1987) [Sov. J. Quantum Electron. **17**, 270 (1987)].

[8]A. I. Pavlovskiĭ and V. I. Karelin, Vestn. Kiev. Univ. No. 29, 115 (1988).

[9]L. B. Loeb, *Fundamental Processes of Electrical Discharge in Gases*, Wiley, N.Y., 1939.

[10]J. M. Meek and J. D. Craggs, *Electrical Breakdown of Gases*, Oxford Univ. Press, London, 1953 [Russ. transl. IL, M., 1960].

[11]H. Raether, *Electron Avalanches and Breakdown in Gases*, Butterworth, London, 1964 [Russ. transl. Mir, M., 1968].

[12]É. D. Lovanskiĭ and O. B. Firsov, *Theory of the Spark* [in Russian], Atomizdat, M., 1975.

[13]A. Przybylski, Z. Phys. **151**, 264 (1958).

[14]T. H. Teich, Z. Phys. **199**, 378 (1967).

[15]W. Sroka, Z. Naturforsch. **23a**, 2004 (1968).

[16]W. Sroka, Z. Naturforsch. **24a**, 398 (1969).

[17]G. W. Penney and G. T. Hummert, J. Appl. Phys. **41**, 572 (1970).

[18]Yu. L. Stankevich, Zh. Tekh. Fiz. **40**, 1476 (1970) [Sov. Phys. Tech. Phys. **15**, 1138 (1971)].

[19]K. Yoshida and H. Tagashira, J. Phys. Ser. D **9**, 491 (1976).

[20]A. P. Broĭtman, O. A. Omaraov, S. A. Reshetnyak, and A. A. Rukhadze, Preprint No. 197, P. N. Lebedev Physics Institute, Academy of Sciences of the USSR, M., 1984.

[21]G. V. Naĭdis, Zh. Tekh. Fiz. **52**, 868 (1982) [Sov. Phys. Tech. Phys. **27**, 555 (1982)].

[22]M. B. Zheleznyak, A. Kh. Mnatsakanyan, and S. V. Sizykh, Teplofiz. Vys. Temp. **20**, 423 (1982). [High Temp. (USSR) **20**, 357 (1982)].

[23]L. P. Babich, I. A. Berezin, T. V. Loĭko, and M. D Tarasov, Izv. Vyssh. Uchebn. Zaved., Radiofiz **25**, 1131 (1982). [Radiophys. Quantum Electron. **25**, 807 (1982)].

[24]P. Strizke, I. Sander, and H. Raether, J. Phys. Ser. D **10**, 2285 (1977).

[25]N. S. Rudenko and V. I. Smetanin, Izv. Vyssh. Uchebn. Zaved., Fiz. No. 7, 34 (1977). [Sov. Phys. J. **20**, 859 (1977)].

[26]L. P. Babich, Fiz. Plazmy 7, 1419 (1981) [Sov. J. Plasma Phys. **7**, 783 (1981)].

[27]L. P. Babich and Yu. L. Stankevich, Zh. Tekh. Fiz. **42**, 1669 (1972) [Sov. Phys. Tech. Phys. **17**, 1333 (1972)].

[28]G. A. Askar'yan, Pis'ma Zh. Eksp. Teor. Fiz. **1**, 44 (1965) [JETP Lett. **1**, 97 (1965)].

[29]G. A. Askar'yan, Pis'ma Zh. Eksp. Teor. Fiz. **2**, 179 (1965) [JETP Lett. **2**, 113 (1965)].

[30]G. A. Askar'yan Tr. Fiz. Inst. Akad. Nauk SSSR **66**, 66 (1973). [Proc. (Tr.) P. N. Lebedev Phys. Inst. Acad. Sci. USSR **66**, (1973)].

[31]Yu. L. Stankevich and V. G. Kalinin, Zh. Tekh. Fiz. **36**, 1499 (1966) [Sov. Phys. Tech. Phys. **11**, 1120 (1967).

[32]L. P. Babich, T. V. Loĭiko, and B. N. Shamraev, Izv. Vyssh. Uchebn. Zaved., Radiofiz. **22**, 100 (1979). [Radiophys. Quantum Electron. **22**, 68 (1979)].

[33]L. P. Babich, T. V. Loĭko, and L. V. Tarasova, Izv. Vyssh. Uchebn. Zaved., Radiofiz. **20**, 637 (1977). [Radiophys. Quantum Electron. **20**, (1977)].

[34]E. E. Kunhardt and W. W. Byszewski, Phys. Rev. Ser. A **21**, 2069 (1980).

[35]L. P. Babich, Dokl. Akad. Nauk SSSR **263**, 76 (1982) [Sov. Phys. Dokl. **27**, 215 (1982)].

[36]L. P. Babich, Fiz. Plazmy **8**, 718 (1982) [Sov. J. Plasma Phys. **8**, 404 (1982)].

[37]G. V. Kolbychev, in: *Proceedings of the Fifteenth International Conference on Phenomena in Ionized Gases* [in Russian], Minsk, 1980, p. 619.

[38]L. P. Babich, N. V. Ivanov, T. V. Loĭko, and L. V. Tarasova, in: *Proceedings of the Third All-Union Conference on the Physics of Gas Discharges* [in Russian], Kiev, 1986, p. 9.

[39]L. P. Babich, T. V. Loĭko, and L. V. Tarasov, in: *Proceedings of the Third All-Union Conference on the Physics of Gas Discharges* [in Russian], Kiev, 1986, p. 11.

[40]V. A. Granovskiĭ, *Electric Currents in Gases, Vol. 2. Steady-State Currents* [in Russian], Nauka, M., 1971.

[41]C. T. R. Wilson, Proc. Cambr. Phil. Soc. **22**, 534 (1925).

[42]S. Frankel, V. Highland, T. Sloan, O. van Dyck, and W. Wales, Nucl. Instrum. Methods **44**, 345 (1966).

[43]Yu. L. Stankevich and V. G. Kalinin, Dokl. Akad. Nauk SSSR **39**, 1530 (1967) Incorrect reference. Probably should be **177**(1), 72 (1967). [Sov. Phys. Dokl. **12**, 1042 (1967)].

[44]R. C. Noggle, E. P. Krider, and J. R. Wayland, J. Appl. Phys. **39**, 4746 (1968).

[45]Yu. I. Bychkov, V. V. Osipov, Yu. A. Kurbatov, and A. G. Filonov, Izv. Vyssh. Uchebn. Zaved., Fiz. No. 1, 61 (1973) [Sov. Phys. J. **16**, 46 (1973)].

[46]É. I. Asinovskiĭ, V. V. Markovets, D. N. Polyakov, A. M. Ul'yanov, and I. V. Filyugin, Teplofiz. Vys. Temp. **23**, 606 (1985).

[47]A. G. Abramov, E. I. Asinovskiĭ, and L. M. Vasilyak, Fiz. Plazmy **14**, 979 (1988) [Sov. J. Plasma Phys. **14**, 575 (1988)].

[48]L. V. Tarasova and L. N. Khudyankova, Zh. Tekh. Fiz. **39**, 1530 (1979) [Sov. Tech. Phys. **14**, 1148 (1969)].

[49]V. V. Kremnev and Yu. A. Kurbatov, Zh. Tekh. Fiz. **42**, 795 (1972) [Sov. Phys. Tech. Phys. **17**, 626 (1972)].

[50]L. V. Tarasova, L. N. Khudayakova, T. V. Loĭko, and V. A. Tsukerman, Zh. Tekh. Fiz. **44**, 564 (1974) [Sov. Phys. Tech. Phys. **19**, 351 (1975)].

[51]L. P. Babich, T. V. Loĭko, L. V. Tarasova, and V. A. Tsukerman, Pis'ma Zh. Tekh. Fiz. **1**, 166 (1975) [Sov. Tech. Phys. Lett. **1**, 79 (1975)].

[52]T. V. Loĭko, L. V. Tarasova, and V. A. Tsukerman, Pis'ma Zh. Tekh. Fiz. **3**, 120 (1977) [Sov. Tech. Phys. Lett. **3**, 48 (1977)].

[53]W. W. Byszewski and G. Reinhold, Phys. Rev. A **26**, 2826 (1982).

[54]L. P. Babich, T. V. Loĭko, and L. V. Tarasova, Zh. Tekh. Fiz. **48**, 1617 (1978) [Sov. Phys. Tech. Phys. **23**, 915 (1978)].

[55]P. N. Dashuk and S. L. Kulakov, Pis'ma Zh. Tekh. Fiz. **5**, 69 (1979) [Sov. Tech. Phys. Lett. **5**, 26 (1979)].

[56]P. A. Bokhan and G. V. Kolbychev, Pis'ma Zh. Tekh. Fiz. **6**, 418 (1980) [Sov. Tech. Phys. Lett. **6**, 180 (1980)].

[57]G. V. Kolbychev and E.A. Samyshki, Zh. Tekh. Fiz. **51**, 2032 (1981) [Sov. Phys. Tech. Phys. **26**, 1185 (1981)].

[58]L. P. Babich, T. V. Loĭko, and L. V. Tarasova, *Proceedings of the Second Symposium on High-Current Electronics* [in Russian], Tomsk, 1975, p. 69.

[59]L. P. Babich, I. A. Berezin, T. V. Loĭko, M. D. Tarasov, L. V. Tarasova, and R. S. Chikina, Zh. Tekh. Fiz. **47**, 195 (1977) [Sov. Phys. Tech. Phys. **22**, 113 (1977)].

[60]L. P. Babich, T. V. Loĭko, and L. V. Tarasova, *Proceedings of the Second All-Union Conference on the Physics of the Electric Breakdown of Gases* [in Russian], Tartu, 1984, p. 250.

[61]L. P. Babich and T. V. Loĭko, Zh. Tekh. Fiz. **55**, 956 (1985) [Sov. Phys. Tech. Phys. **30**, 574 (1985)].

[62]A. I. Pavlovskiĭ, L. P. Babich, T. V. Loĭko, and L. V. Tarasova, Dokl. Akad. Nauk SSSR **281**, 1359 (1985) [Sov. Phys. Dokl. **30**, 303 (1985)].

[63]T. V. Loĭko, Zh. Tekh. Fiz. **50**, 392 (1980) [Sov. Phys. Tech. Phys. **25**, 232 (1980)].

[64]V. S. Bosamykin, V. I. Karelin, A. I. Pavlovskiĭ, and P. B. Repin, Pis'ma Zh. Tekh. Fiz. **6**, 885 (1980) [Sov. Tech. Phys. Lett. **6**, 383 (1980)].

[65]D. P. Whitmire, Lett. Nuovo Cim. **26**, 497 (1979).

[66]A. V. Gurevich, Zh. Eksp. Teor. Fiz. **39**, 1296 (1960) [Sov. Phys. JETP **12**, 904 (1961)].

[67]L. P. Babich and Yu. V. Petrov, Fiz. Plazmy **3**, 832 (1977) [Sov. J. Plasma Phys. **3**, 469 (1977)].

[68]L. R. Peterson and A. E. S. Green, J. Phys. Ser. B **1**, 1131 (1968).

[69]A. E. S. Green and L. R. Peterson, J. Geophys. Res. **73**, 233 (1968).

[70]T. W. Shyn, R. S. Stolarski, and G. R. Carignan, Phys. Rev. Ser. A **6**, 1002 (1972).

[71]G. D. Alkhazov, Zh. Tekh. Fiz. **44**, 1044 (1974) [Sov. Phys. Tech. Phys. **19**, 658 (1974)].

[72]E. E. Kunhardt, Y. Tzeng, and J. P. Boeuf, Phys. Rev. Ser. A **34**, 440 (1986).

[73]N. V. Belkin, N. I. Komyak, E. N. Peliks, and V. A. Tsukerman, Prib. Tekh. Eksp. No. 2, 194 (1972). [Instrum. Exp. Tech. (USSR) **15**, 535 (1972)].

[74]L. P. Babich, T. V. Loĭko, and L. V. Tarasova, Prib. Tekh. Eksp. No. 1, 203 (1977) [Instrum. Exp. Tech. (USSR) **20**, 233 (1977)].

[75]Yu. I. Bychkov, Yu. D. Korolev, and P. A. Gavrilyuk, Zh. Tekh. Fiz.

42, 1674 (1972) [Sov. Phys. Tech. Phys. 17, 1337 (1972)].
[76] S. I. Andreev and G. M. Novikova, Zh. Tekh. Fiz. 45, 1692 (1975) [Sov. Phys. Tech. Phys. 20, 1078 (1975)].
[77] H. H. Seliger, Phys. Rev. 100, 1059 (1955).
[78] L. P. Babich and T. V. Loĭko, Prib. Tekh. Eksp. No. 2, 188 (1989). [Instrum. Exp. Tech. (USSR) 32, 468 (1989)].
[79] L. P. Babich, Zh. Tekh. Fiz. 42, 1617 (1972) [Sov. Phys. Tech. Phys. 17, 1292 (1972)].
[80] R. B. Baksht, Yu. D. Korolev, and G. A. Mesyats, Fiz. Plazmy 3, 652 (1977) [Sov. J. Plasma Phys. 3, 369 (1977)].
[81] Yu. D. Korolev, V. A. Kuz'min, G. A. Mesyats, and V. P. Rotshteĭn, Zh. Tekh. Fiz. 49, 410 (1979) [Sov. Phys. Tech. Phys. 24, 236 (1979)].
[82] G. F. Kolbychev, Zh. Tekh. Fiz. 52, 511 (1982) [Sov. Phys. Tech. Phys. 27, 326 (1982)].
[83] H. Schlumbohm, Z. Phys. 182, 316 (1965); 184, 491 (1965).
[84] L. P. Babich, Zh. Tekh. Fiz. 44, 1846 (1974) [Sov. Phys. Tech. Phys. 19, 1154 (1974)].
[85] L. P. Babich, Izv. Vyssh. Uchebn. Zaved., Radiofiz. 28, 236 (1985). [Radiophys. Quantum Electron. 28, 163 (1985)].
[86] Yu. P. Konyushaya, *Discoveries by Soviet Scientists* [in Russian], Mosk. rabochiĭ, M., 1979.
[87] G. A. Mesyats, Pis'ma Zh. Tekh. Fiz. 1, 885 (1975) [Sov. Tech. Phys. Lett. 1, 385 (1975)].
[88] L. P. Babich and M. D. Tarasov, Izv. Vyssh. Uchebn. Zaved., Radiofiz. 23, 1365 (1980). [Radiophys. Quantum Electron. 233, 914 (1980)].
[89] L. P. Babich, Izv. Vyussh. Uchebn. Zaved., Radiofiz. 18, 1056 (1975). [Radiophys. Quantum Electron. 18, (1975)].
[90] V. V. Kremnev and G. A. Mesyats, Zh. Prikl. Mekh. Tekh. Fiz. No. 1, 40 (1971). [J. Appl. Mech. Tech. Phys. (1971)].
[91] E. E. Kunhardt, *Electric Breakdown and Discharges in Gases: Proceedings of NATO Advanced Study Institute*, Les Arcs, 1981, N.Y., 1983, Pt. A, p. 241.
[92] G. A. Mesyats and Yu. I. Bychkov, Zh. Tekh. Fiz. 37, 1712 (1967) [Sov. Phys. Tech. Phys. 12, 1255 (1967)].
[93] L. G. Bychkova, Yui. I. Bychkov, and G. A. Mesyats, Izv. Vyssh. Uchebn. Zaved., Fiz. No. 2, 36 (1969). [Sov. Phys. J. 12, 162 (1969)].
[94] L. P. Babich and B. N. Shamraev, Zh. Tekh. Fiz. 55, 1170 (1985) [Sov. Phys. Tech. Phys. 30, 668 (1985)].
[95] Yu. E. Kreĭndel', *Plasma Sources of Electrons* [in Russian], Atomizdat, M., 1977.
[96] K. N. Ul'yanov, Teplofiz. Vys. Temp. 18, 682 (1980).
[97] A. I. Danilevich, in: *Proceedings of the Fourth All-Union Symposium on High-Current Electronics*, Vol. 1 [in Russian], Tomsk, 1982, p. 123.
[98] L. Yu. Dzagurov, A. V. Zharinov, *et al.*, *Proceedings of the Fourth All-Union Symposium on High-Current Electronics*, Vol. 1 [in Russian], Tomsk, 1982, p. 111.

Translated by D. Parsons